Journal of Ethnopharmacology 333 (2024) 118484

Contents lists available at ScienceDirect

Journal of Ethnopharmacology

journal homepage: www.elsevier.com/locate/jethpharm

Er-Dong-Xiao-Ke decoction regulates lipid metabolism via PPARG-mediated UCP2/AMPK signaling to alleviate diabetic meibomian gland dysfunction

Li Shi [a,1], Liu-Jiao Li [a,1], Xin-Yi Sun [b,1], Yi-Ying Chen [c], Dan Luo [a], Lu-Ping He [a], Hui-Jie Ji [a], Wei-Ping Gao [a,**], Hu-Xing Shen [a,*]

[a] Department of Ophthalmology, The Affiliated Hospital of Nanjing University of Chinese Medicine, Jiangsu Province Hospital of Chinese Medicine, Nanjing, Jiangsu, PR China
[b] Department of Endocrinology, The Affiliated Hospital of Nanjing University of Chinese Medicine, Jiangsu Province Hospital of Chinese Medicine, Nanjing, Jiangsu, PR China
[c] Department of Acupuncture Rehabilitation, The Affiliated Hospital of Nanjing University of Chinese Medicine, Jiangsu Province Hospital of Chinese Medicine, Nanjing, Jiangsu, PR China

ARTICLE INFO

Handling Editor: Dr. K Shaari

Keywords:
Meibomian gland dysfunction
Type 2 diabetes mellitus
Er-Dong-Xiao-Ke decoction
Lipid metabolism
Peroxisome proliferator-activated receptor gamma

ABSTRACT

Ethnopharmacological relevance: Meibomian gland dysfunction (MGD), complicated by type 2 diabetes, is associated with a high incidence of ocular surface disease, and no effective drug treatment exists. Diabetes mellitus (DM) MGD shows a notable disturbance in lipid metabolism. Er-Dong-Xiao-Ke decoction (EDXKD) has important functions in nourishing yin, clearing heat, and removing blood stasis, which are effective in the treatment of DM MGD.

Aim of the study: To observe the therapeutic effect of EDXKD on DM MGD and its underlying molecular mechanism.

Materials and methods: After establishing a type 2 DM (T2DM)-induced MGD rat model, different doses of EDXKD and T0070907 were administered. The chemical constituents of EDXKD were identified by liquid chromatography-tandem mass spectrometry (LC-MS/MS), and the molecular mechanism of EDXKD in treating DM MGD was predicted using network pharmacology. Lipid metabolism in DM meibomian glands (MGs) was analyzed using LC-MS/MS, and lipid biomarkers were screened and identified. Histological changes and lipid accumulation in MGs were detected by staining, and Peroxisome proliferator-activated receptor gamma (PPARG) expression in MG acinar cells was detected by immunofluorescence. The expression of lipid metabolism-related factors was detected by reverse transcription-quantitative polymerase chain reaction (RT-qPCR) or western blotting.

Results: EDXKD reduced lipid accumulation in the MGs and improved the ocular surface index in DM MGD rats. The main active components of EDXKD had advantages in lipid regulation. Additionally, the PPARG signaling pathway was the key pathway of EDXKD in the treatment of DM MGD. Twelve lipid metabolites were biomarkers of EDXKD in the treatment of DM MGD, and glycerophospholipid metabolism was the main pathway of lipid regulation. Moreover, EDXKD improved lipid deposition in the acini and upregulated the expression of PPARG. Further, EDXKD regulated the PPARG-mediated UCP2/AMPK signaling network, inhibited lipid production, and promoted lipid transport.

Conclusion: EDXKD is an effective treatment for MGD in patients with T2DM. EDXKD can regulate lipids by regulating the PPARG-mediated UCP2/AMPK signaling network, as it reduced lipid accumulation in the MGs of DM MGD rats, promoted lipid metabolism, and improved MG function and ocular surface indices.

Abbreviations: MGs, Meibomian glands; MGD, Meibomian gland dysfunction; DM, diabetes mellitus; PPARG, Peroxisome proliferator-activated receptor gamma; MTTP, Microsomal triglyceride transporter protein; APOB, Apolipoprotein-B; UCP2, Uncoupling protein 2; AMPK, AMP-activated protein kinase; ACC, Acetyl-CoA carboxylase.

* Corresponding author.
** Corresponding author.
E-mail addresses: 260790@njucm.edu.cn (W.-P. Gao), polaris_86@163.com (H.-X. Shen).

[1] These authors have contributed equally to this work.

https://doi.org/10.1016/j.jep.2024.118484
Received 4 April 2024; Received in revised form 6 June 2024; Accepted 20 June 2024
Available online 24 June 2024

1. Introduction

Meibomian glands (MGs), which are holocrine sebaceous glands embedded between the upper and lower tarsi of the eyelid, synthesize, store, and secrete lipids (Jester et al., 1981). MGs play a key role in maintaining the homeostasis of the ocular surface. Secreted eyelid esters contribute to the composition of the lipid layer of the tear film, maintaining the stability of the tear film to prevent tear evaporation and forming a barrier to protect the ocular surface from microorganisms and organic matter (Sabeti et al., 2020). Meibomian gland dysfunction (MGD) is a group of chronic functional abnormalities of the MGs, characterized by hyposecretion, hypersecretion, or obstruction of the MGs, quality or quantity alterations of the meibum, and eventual acinar atrophy and gland dropout (Nelson et al., 2011). MGD is the most common cause of dry eye and seriously affects the quality of life of patients (Chhadva et al., 2017).

Type 2 diabetes is a common chronic metabolic disease that causes not only persistent hyperglycemia but also disorders of lipid metabolism (Wang et al., 2022). When glycosylated hemoglobin levels were ≥7%, the MG function of patients with diabetes was more likely to be abnormal, with other characteristics including a larger missing area of MGs, atrophy of acini, decreased acinar unit density, and severe lipid deposition (Fan et al., 2021; Yu et al., 2019). *In vitro*, lipid accumulation was significant in organic mouse MGs cultured with high glucose (Zou et al., 2022). Furthermore, analysis of the lipid composition of MGs revealed that diabetes can affect the lipid expression of MGs and exacerbate the progression of MGD (Yang et al., 2021). Evidence from these studies suggests that lipid metabolism disorders triggered by diabetes are key factors in the development of MGD. Currently, treatment options for type 2 diabetes mellitus (T2DM) MGD have some limitations. Physiotherapies, such as meibomian gland massage and intense pulsed light, are commonly used to improve symptoms; however, a certain recurrence rate persists (Blackie et al., 2015; Cote et al., 2020). Additionally, the local use of drugs, such as artificial tears and anti-inflammatory agents, merely relieves the symptoms of dry eye complicated by MGD (Sabeti et al., 2020) and cannot fundamentally solve the problem, with long-term use causing drug-induced keratitis and aggravating the symptoms of dry eye (Vernhardsdottir et al., 2022).

Peroxisome proliferator-activated receptor gamma(PPARG) is an important regulator of glucose and lipid metabolism (Berger and Moller, 2002). In combination with adiponectin and other molecules, PPARG activation can improve glucose metabolism and relieve insulin resistance (Habtemichael et al., 2021; Ziemke and Mantzoros, 2010). In addition, PPARG regulates insulin-induced adipogenesis and is an important regulator of lipid synthesis and sebaceous gland function (Mastrofrancesco et al., 2017). Furthermore, PPARG plays a key role in MG lipid metabolism, and PPARG agonists can promote meibomian cell differentiation and lipid metabolism (Phan et al., 2022). Therefore, exploring lipid regulation mediated by the PPARG signaling pathway has unique prospects for the treatment of diabetes mellitus (DM) MGD.

Er-Dong-Xiao-Ke Decoction (EDXKD) (Patent No. CN116637154A) is an approved compound preparation developed by the Affiliated Hospital to Nanjing University of Chinese Medicine. EDXKD has high clinical efficacy and safety, exerts anti-inflammatory effects, and regulates glucose metabolism, relieving the symptoms of dry eye and restoring MG function in patients with diabetes (Sun et al., 2024; Zhu, 2020). Similarly, our previous study using a streptozocin (STZ)-induced T2DM rat model demonstrated that EDXKD ameliorated diabetic dry eye and meibomian gland symptoms (Li et al., 2023a). However, the molecular mechanism of EDXKD in the treatment of DM MGD remains unclear and requires further investigation. Hence, in this study, we established an STZ-induced T2DM MGD rat model to evaluate whether EDXKD regulates lipid metabolism through the PPARG signaling pathway to treat DM MGD.

Table 1
Formula of the Er-Dong-Xiao-Ke decoction.

Latin name	Chinese name	Amount (g)	Plant part
Asparagus cochinchinensis	天冬 Tiandong	10	Root
Ophiopogon japonicus (Thunb.) Ker Gawl.	麦冬 Maidong	10	Root
Trichosanthes kirilowii Maxim.	天花粉 Tianhuafen	10	Root
Dioscorea opposita Thunb.	山药 Shanyao	15	Root
Pueraria lobata (Willd.) Ohwi	葛根 Gegen	15	Root
Prunella vulgaris	夏枯草 Xiakucao	10	Fruit ear
Coptis chinensis	黄连 Huanglian	3	Rhizome
Dendrobium nobile	石斛 Shihu	10	Stem
Bidens pilosa L.	鬼针草 Guizhencao	30	Stem

2. Materials and methods

2.1. Drug preparation

EDXKD comprises nine medicines, and their medicinal dosages are shown in Table 1. The drug formulation particles were provided by the Affiliated Hospital of Nanjing University of Chinese Medicine and were dissolved in heated distilled water and prepared as a solution with a drug concentration of 1.1 g/mL.

2.2. Liquid chromatography-tandem mass spectrometry preparation and analysis (LC-MS/MS)

The EDXKD samples were placed in an automatic sampler at 4 °C during the whole analysis process, and the composition of EDXKD was analyzed by SHIMADZU-LC30 ultra-high performance liquid chromatography (UHPLC). LC-MS/MS analysis was performed with ACQUITY UPLC® HSS T3 column (2.1 × 100 mm, 1.8 μm) (Waters, Milford, MA, USA). The mobile phase consisted of two components—A: 0.1% formic acid in water; and B: acetonitrile. The chromatographic gradient elution procedure was as follows: 0–2 min, 0% B; 2–6 min, 0–48% B; 6–10 min, 8–100% B; 10–12 min, 100% B; 12–12.1 min, 100–0% B; and 12.1–15 min, 0% B. The samples were separated using UHPLC and analyzed using a QE Plus mass spectrometer (Thermo Scientific, spectrometer, USA). A heated electrospray ionization (HESI) source was used for ionization, and the ionization conditions were as follows: spray voltage at 3.8 kv(+) and 3.2 kv(−); capillary temperature at 320(±); sheath gas at 30(±); aux gas at 5(±); probe heater temperature at 350(±); and s-lens radiofrequency level at 50. The original data were calibrated using MSDIAL software for peak alignment, retention time correction, and peak area extraction.

2.3. Mechanism of EDXKD in the treatment of DM MGD based on network pharmacology

Combined with the results of the LC-MS/MS analysis, the effective chemically active substances in EDXKD were screened using the integrated traditional Chinese medicine (ITCM) (http://itcm.biotcm.net/), herbal ingredients' targets (HERB) (http://herb.ac.cn/), and traditional Chinese medicine systems pharmacology (TCMSP) (http://tcmspw.com) databases. The obtained active ingredients will be imported into SwissTargetPrediction (http://swisstargetprediction.ch) to predict their targets, selecting those with a Score >0 as potential targets of EDXKD. The disease targets of T2DM and MGD will be queried using the Online Mendelian Inheritance in Man (OMIM) (http://www.omim.org/), GeneCards (https://www.genecards.org/), and Disease Gene Network

Table 2
Primer sequences.

Gene	Forward primers (5′–3′)	Reverse primer (5′–3′)
β-Actin	AGATTACTGCCCTGGCTCCTAG	CATCGTACTCCTGCTTGCTGAT
PPARG	TCCCGTTCACAAGAGCTGAC	ATAATAAGGCGGGGACGCAG
UCP2	AGATGTGGTAAAGGTCCGCTTC	GCAATGGTCTTGTAGGCTTCG
CD36	ACATTTGCAGGTCTATCTACG	AATGGTTGTCTGGATTCTGG
APOB	CGTGGGCTCCAGCATTCTA	TCACCAGTCATTTCTGCCTTTG
MTTP	AGTCACGATAACGGCTGTCAATGTC	GCCTCCAAGTTGTCCTTTCCTACG

(DisGeNET) (http://www.disgenet.org) databases. Targets with a Score >0 will be selected, and the target of EDXKD intervention in T2DM and MGD will be determined using Venny. Subsequently, a network map of the herb compound targets will be constructed using Cytoscape 3.10.1. We imported the obtained intersection targets into STRING 12.0 (https://string-db.org) to construct the PPI network. The minimum required interaction score was set to 0.4 to finalize the PPI network. To further identify hub genes, the PPI network was imported into Cytoscape 3.10.1. The degree scores of each node in the PPI network were calculated using the CytoHubba plugin, and the top 10 hub genes were selected to construct the Hub Gene network. Subsequently, to understand the potential pathways of EDXKD intervention in T2DM MGD, we performed GO and KEGG enrichment analysis of all intersecting genes using the clusterProfiler package in R. The false discovery rate (FDR) was calculated using the Benjamini-Hochberg Procedure (BH) method, with a threshold of FDR <0.05. We then selected the top 10 GO and KEGG annotations that met this criterion and visualized them using the ggplot2 packages. Finally, using Cytoscape 3.10.1, we constructed a "Herb-Target-Component-Pathway" network by integrating the obtained KEGG pathways with the components, targets, and herbs, and analyzed this network.

2.4. Animals

Healthy male Sprague-Dawley rats weighing 200–220 g were purchased from the Experimental Animal Center of Nantong University and raised in the Pharmacology Laboratory of Jiangsu Province Hospital of Chinese Medicine. All animal experiments were approved by the Animal Care and Use Committee of Nanjing University of Traditional Chinese Medicine (Approval Number: 2021DW0201). The experimental animals were housed in ambient conditions (room temperature, 22 ± 2 °C; relative humidity, 60 ± 5%; and an alternating 12-h light-dark cycle). Prior to the experiment, the anterior segment of the eyes of all animals was examined and found to have no abnormality; the tear flow strip was greater than 7 mm/20 s, and MGs had no abnormality.

2.5. Animal grouping and treatment

After 1 week of adaptive feeding, the rats were randomly divided into control, model, low-dose, middle-dose, and high-dose groups, with five rats per group. According to the previous experimental experience and the dose conversion algorithm, a dose of 11 g/kg was designated as EDXKD-M, which is equivalent to the clinical dose for humans (Li et al., 2023a). The doses of 5.5 g/kg and 22 g/kg of EDXKD were designated as EDXKD-L and EDXKD-H, respectively. The control group was fed standard feed, and all other groups were fed a high-fat diet (basic feed+10% lard+10% sucrose+5% cholesterol). After 4 weeks of feeding, all rats were fasted for 12 h. Except for the control group, all other groups were injected intraperitoneally with STZ (30 mg/kg, S0130-1G, Sigma, USA) dissolved in sodium citrate buffer. The control group was intraperitoneally injected with an equal volume of sodium citrate buffer. Fasting blood glucose was measured on days 3, 7, and 14 the after injection. A fasting blood glucose level of ≥16.7 mmol/L was used to model T2DM (Almugadam et al., 2021). Subsequently, MGD was induced in T2DM rats for 8 weeks (Furman, 2021). The low-, middle-, and high-dose groups were treated with EDXKD, whereas the control and model groups were treated with an equal volume of normal saline once a day for 4 weeks. The rats were anesthetized with isoflurane (R510-22, Shanghai Yuyan Instruments Co., Ltd., China). MG tissue was isolated from 2 mm of the palpebral margin, and blood was collected for further analysis.

To further clarify the mechanisms of EDXKD and PPARG in the treatment of DM MGD, we used PPARG antagonist T0070907 (2 mg/kg/d, S2871, Selleckchem, USA) to suppress the expression of PPARG in rats by intraperitoneal injection (Li et al., 2021). Based on the above experiments, we determined the optimal therapeutic concentration of EDXKD. Healthy rats were randomly divided into control, model, EDXKD, T0070907, and EDXKD + T0070907 groups, with five rats per group. After 12 weeks, the rats were intragastrically or intraperitoneally injected for 4 weeks. Rats were anesthetized with isoflurane, and MGs and blood were collected for further analysis.

2.6. Fasting blood glucose monitoring

After STZ injection, the rats were weighed every 2 weeks, and fasting blood glucose levels were measured by sampling the tail vein.

2.7. MGD-related indicators data collection

2.7.1. Tear break-up time (BUT)

Sodium fluorescein staining test paper (Liaoning Meizilin Pharmaceutical Co., Ltd., China) was soaked in the lower eyelid fornix, resulting in an even distribution of fluorescein on the cornea after blinking. The first corneal dry spot was observed using a handheld slit-lamp microscope (SL-D301; Topcon, Tokyo, Japan) under cobalt blue light.

2.7.2. Corneal fluorescein staining score (FL)

Corneal epithelial damage was observed using cobalt blue light following the distribution of fluorescein sodium on the cornea. The single-eye cornea was divided into four quadrants on average. A grading scale was applied as follows: 0 indicated non-fluorescent green spots, 1 indicated less than 30 fluorescent green spots, 2 indicated more than 30 spots without fusion sheets, and 3 indicated the presence of staining spots. The sum of the scores in the four quadrants was calculated as the single-eye corneal fluorescein staining score (Wu et al., 2020).

2.7.3. Phenol red thread test (PRT)

After corneal fluorescein sodium staining, the stained end of a phenol cotton thread (Liaoning Meizilin Pharmaceutical Co., Ltd., China) was placed in the lower eyelid near one-third of the lateral canthus of the rats. After the eyes were closed for 20 s, the cotton thread was removed, and the length of the tear staining was measured (Fakih et al., 2019).

2.7.4. Observation of MGs

Under isoflurane anesthesia, the upper and lower eyelids of the rats were rotated, and the structure of the MGs and their orifices were observed using a body microscope (7045P-38 MP, Beijing, China).

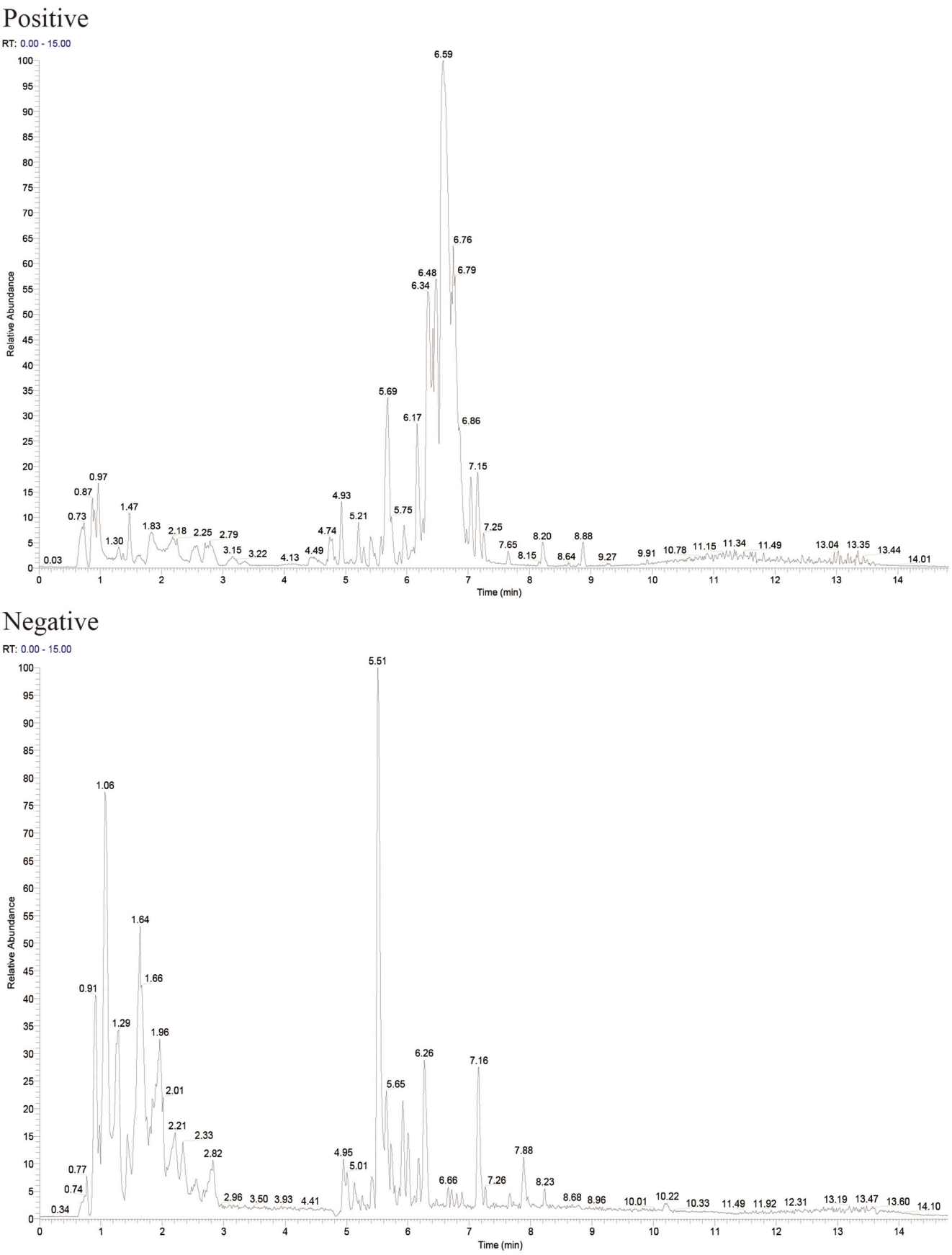

Fig. 1. Chromatograms of EDXKD. EDXKD; Er-Dong-Xiao-Ke decoction.

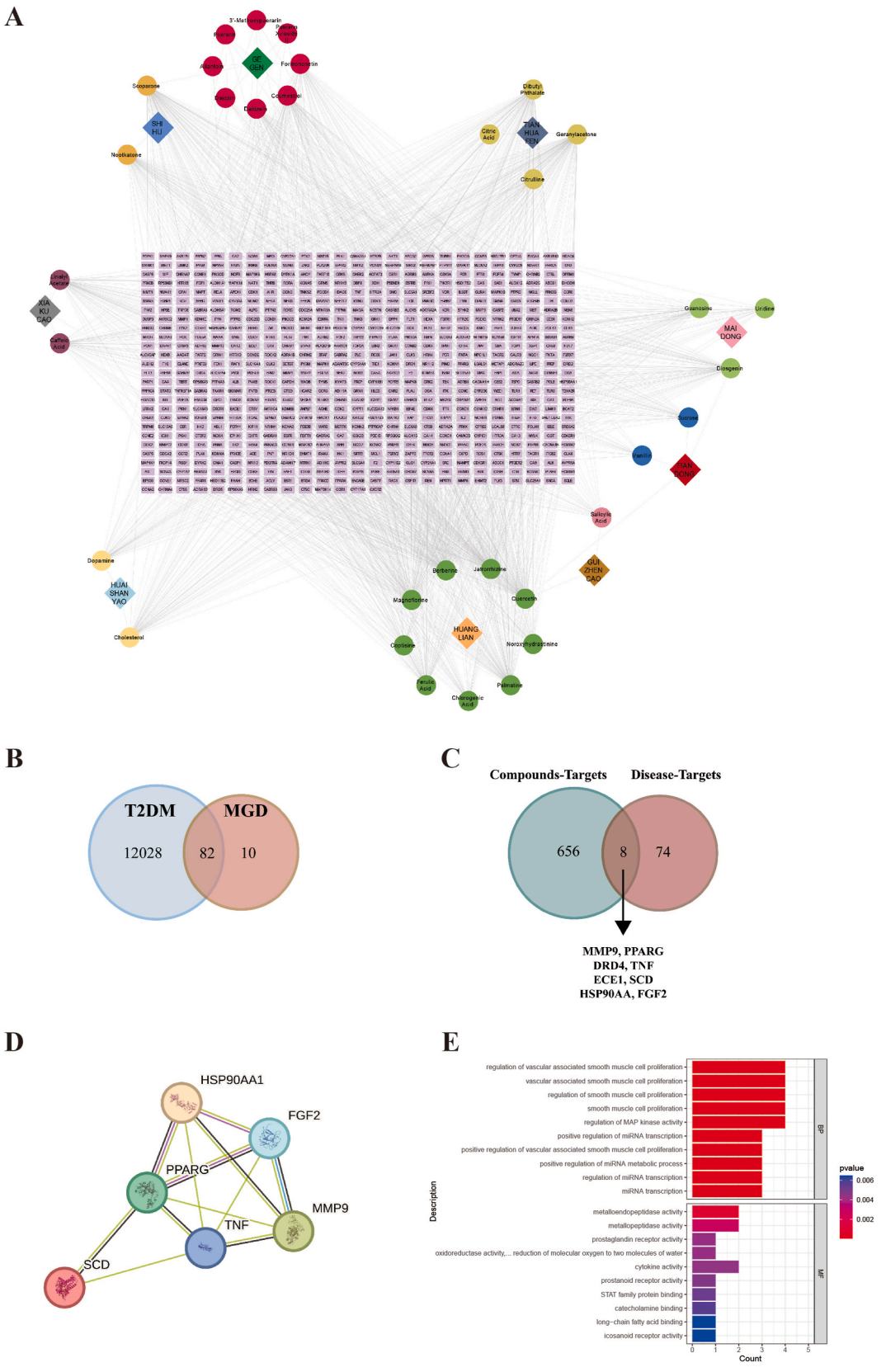

Fig. 2. Analysis of Network pharmacology. (A) network diagrams of active components and potential targets of Er-Dong-Xiao-Ke Decoction (EDXKD); (B) Venn of comorbid genes between type 2 diabetes mellitus (T2DM) and meibomian gland dysfunction (MGD); (C) screening of potential targets for EDXKD treatment of diabetes mellitus (DM) MGD; (D) Protein-protein interaction (PPI) network of potential targets for EDXKD; (E) Gene Ontology (GO) enrichment analysis of targets for EDXKD therapy in DM MGD; (F) visualization of Kyoto Encyclopedia of Genes and Genomes (KEGG) channel annotation analysis results; (G) KEGG enrichment analysis of EDXKD targets; (H) network diagrams of Herb-Target-Component-Pathway.

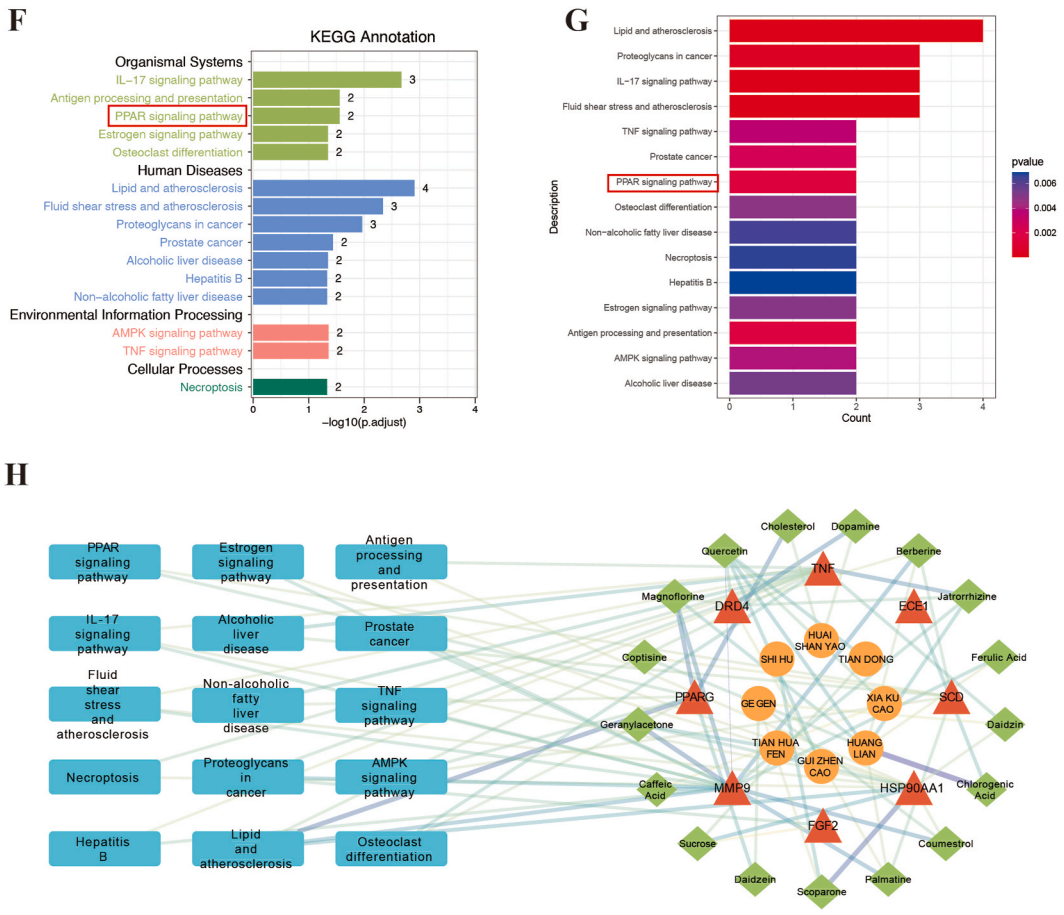

Fig. 2. (*continued*).

2.8. Lipidomics profiling

MG tissue samples were thawed at 4 °C, and 20 mg of each sample was added to 200 μL of pre-cooled butanol/methanol solution (1/1, v/v) containing 10 mmol/L ammonium formate. The samples were vortexed and shaken thoroughly. After ultrasonic extraction for 60 min in an ice bath and centrifugation for 20 min at 4 °C at 16,000×*g*, a suitable amount of supernatant was injected for analysis. An equal amount of samples was mixed into quality control (QC) samples, which were used to determine the instrument status and equilibrium system before injection and to evaluate the stability of the system during the entire experiment.

Throughout the analysis, the samples were placed in a 4 °C autosampler and analyzed on a UHPLC system with a Hypersil GOLD™ C18 column (2.1 × 100 mm, 3 μm). The injection volume was 8 μL, the column temperature was 40 °C, and the flow rate was 0.3 mL/min. Mobile phase A comprised 0.77 g of ammonium formate and an acetonitrile aqueous solution (acetonitrile: water = 6:4, v/v). Mobile phase B comprised an acetonitrile and isopropanol solution (acetonitrile: isopropanol = 1:9, v/v). Mass spectra were obtained using a Q Exactive Plus mass spectrometer in electrospray ionization (ESI) positive and negative ion modes. To avoid the influence of fluctuations in the instrument detection signal, a random sequence was used for continuous analysis of the samples. One QC sample was set up for every 5–10 experimental samples in the sample queue and was used to monitor and evaluate the stability of the system and the reliability of the experimental data. The lipids were identified and quantified using MSDAIL software.

2.9. Measurements of blood lipid level

Serum levels of total cholesterol (TC), triglycerides (TG), high-density lipoprotein (HDL), and low-density lipoprotein (LDL) were measured using an automatic biochemical analyzer (BK-280, BIOBASE, China) and kits (70901, 70902, 70903, 70904, BIOBASE, China).

2.10. Histopathology of MGs

The eyelid tissue was fixed with 4% paraformaldehyde, dehydrated, and embedded in paraffin or another compound at the optimal cutting temperature. Paraffin-embedded sections were stained with hematoxylin and eosin (H&E) to observe structural changes in MGs, while frozen sections were stained with Oil Red O to detect lipid deposition. The pathological changes in each group were observed using CaseViewer 2.4.0 digital microscope, and the ImageJ software was used for subsequent quantitative image analysis.

2.11. Immunofluorescence staining

The slices were prepared as described in 2.10. The slices were heated at 62 °C for 1 h, dewaxed with xylene, and washed with ethanol and water. A hydrogen peroxide-blocking solution was added at 24 °C to inhibit endogenous peroxidase activity. After repairing the heat antigen, the specimen was washed three times with phosphate buffered saline (PBS) for 5 min each. The slices were incubated with a PPARG antibody (1:200, ab41928, Abcam) overnight at 4 °C. The following day, the slices were washed with PBS and incubated at 37 °C for 30 min with corresponding secondary antibodies. After another round of washing with PBS, try-488 tyramine conversion reagent (Bry-try 488, Runnerbio,

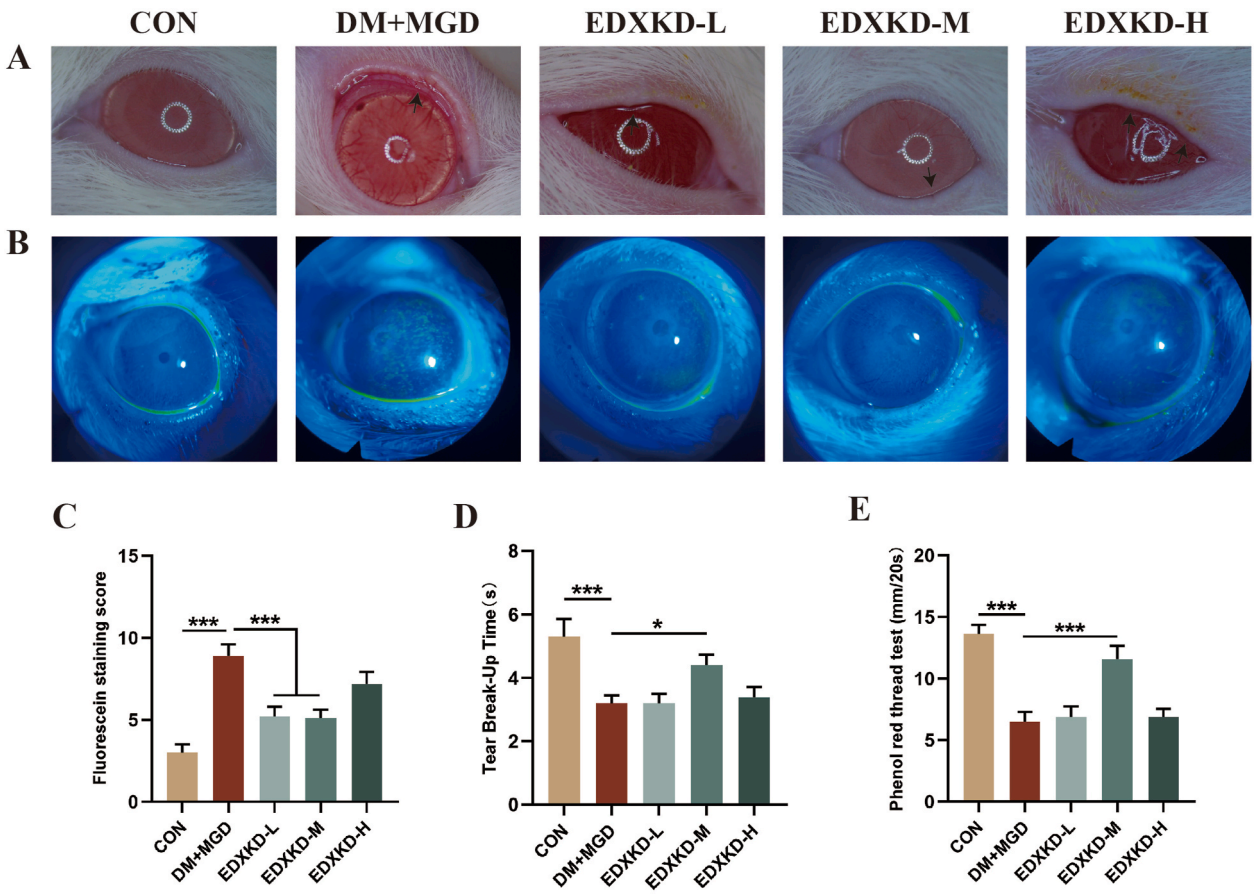

Fig. 3. Manifestation of the eyelid and ocular surface of rats with diabetes. (A) observation of the eyelid performance of each group, the black arrow showed abnormal lipid secretion or unsmooth palpebral margin of meibomian glands (MGs) opening; (B) fluorescein staining images of the cornea in each group; (C) fluorescein staining score of each group; (D) tear break-up time and phenol red thread test (E) of each group. (For interpretation of the references to colour in this figure legend, the reader is referred to the Web version of this article.)

China) was added and incubated at room temperature for 30 min. Finally, a DAPI-containing anti-fluorescence quenching blocking tablet was added. The pathological changes in each group were observed by CaseViewer 2.4.0 digital microscope, and the ImageJ software was used for subsequent quantitative image analysis.

2.12. Western blotting

The MG tissue proteins from rats in each group were extracted and quantified using a BCA kit (P0012, Beyotime, China). The protein on the polyacrylamide gel electrophoresis (PAGE) gel was transferred to a polyvinylidene fluoride (PVDF) membrane, sealed with 5% skim milk, and incubated overnight in β-Actin (1:3000, AF7018, Affinity Biosciences), PPARG (1:1000, ab41928, Abcam), UCP2 (1:1000, 11081-1-AP, Proteintech), AMPK (1:1000, 10929-2-AP, Proteintech), p-AMPK (1:1000, AF3423, Affinity Biosciences), ACC (1:1000, #3676, CST), p-ACC (1:1000, #11818, CST), and CD36 (1:500, #74002, CST) antibodies at 4 °C. The following day, secondary antibodies from rabbit (1:50000, HA1001, HUABIO) or mouse (1:20000, HA1006, HUABIO) were incubated at 24 °C for 1 h. Western blotting was performed with a hypersensitive enhanced chemiluminescence (ECL) photoluminescence solution.

2.13. Ribonucleic acid (RNA) extraction and reverse transcription-quantitative polymerase chain reaction (RT-qPCR)

Total RNA was extracted from MG tissues using an RNA extraction kit (RC101, Vazyme, China). An equal amount of RNA was reverse-transcribed into complementary deoxyribonucleic acid (cDNA) using a reverse transcription kit (R323, Vazyme, China), and RT-qPCR was performed using light quantitative PCR (7500fast, ABI, USA). Primer sequences are listed in Table 2.

2.14. Statistical analysis

The experimental data were analyzed using GraphPad Prism 8.0 software, and the results were expressed as mean ± standard error of the mean (SEM). Statistical differences among groups were analyzed using single-factor analysis of variance (ANOVA). *$p < 0.05$, **$p < 0.01$, and ***$p < 0.01$ were considered statistically significant.

3. Results

3.1. LC-MS/MS analysis of EDXKD

A total of 556 chemical components were identified. A chromatogram of the superimposed extraction ion current is shown in Fig. 1. The retention time, molecular formula, peak intensity, and compound names are provided in Supplementary Material.

The chemical active substances of nine kinds of traditional Chinese medicine in EDXKD were searched through the ITCM, HERB, and TCMSP databases. Combined with the results of the LC-MS/MS analysis, 33 effective chemical constituents were identified, including isoflavone glycosides, berberine, and terpenoids (Supplementary Material).

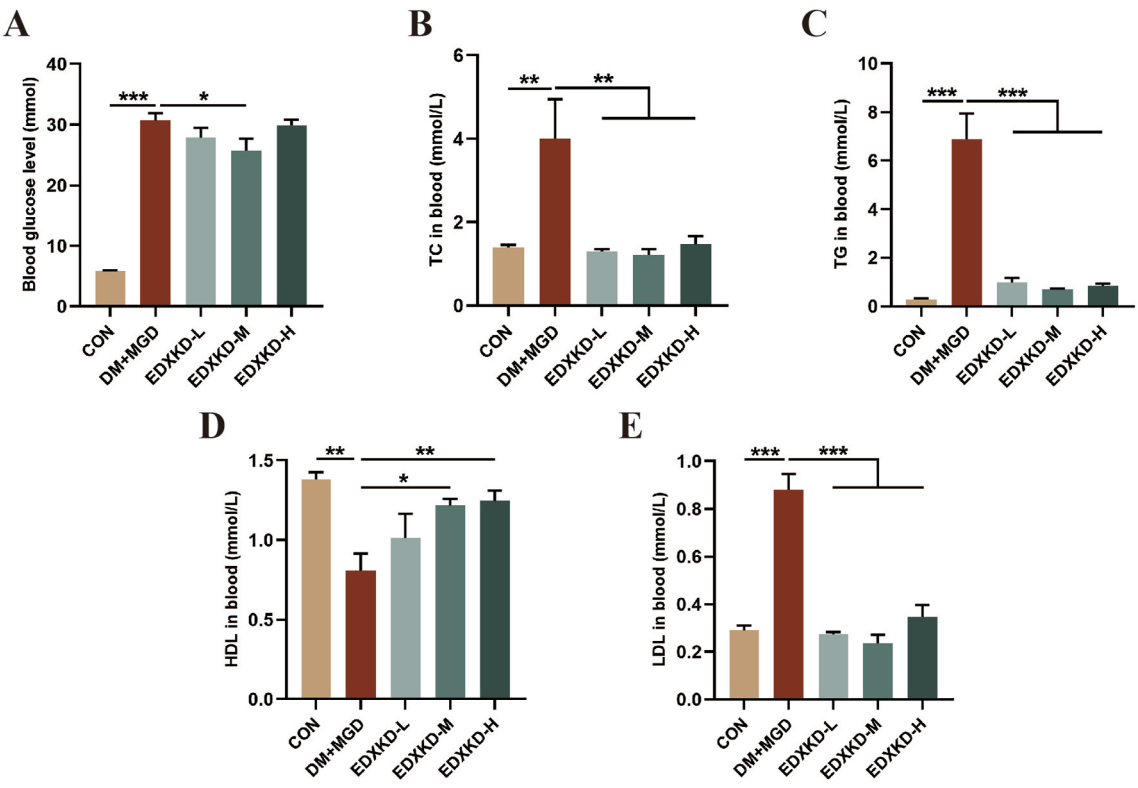

Fig. 4. Levels of glucose and lipids in blood. (A) blood glucose level; (B) total cholesterol (TC); (C) triglyceride (TG); (D) high-density lipoprotein (HDL); and (E) low-density lipoprotein (LDL) in blood.

3.2. Mechanism of EDXKD in the treatment of DM MGD based on network pharmacology

First, 664 potential drug targets were obtained from the 33 identified compounds, and a network map of the herb-compound targets was constructed (Fig. 2A). After querying the disease targets of T2DM and MGD, 82 common disease targets were obtained. These 82 disease targets were considered potential therapeutic targets for DM MGD (Fig. 2B). By integrating the disease and pharmaceutical targets of EDXKD, eight genes may be targeted to play a pharmacological role in the treatment of DM MGD, including MMP9, PPARG, DRD4, TNF, ECE1, SCD, HSP90AA1, and FGF2 (Fig. 2C). The PPI network constructed from the eight targets yielded six nodes via network analysis (Fig. 2D). By calculating the degree of connectivity within the network, the top three hub genes were TNF, PPARG, and MMP9.

In the GO enrichment analysis, 758 enrichment results were obtained ($p < 0.05$, $q < 0.05$), comprising 730 items related to biological processes and 28 items related to molecular functions (Fig. 2E). Additionally, 15 relevant pathways were enriched in the KEGG enrichment analysis. Annotation analysis of these pathways showed that the KEGG pathways were dominated by human diseases and organismal systems (Fig. 2F). Further visualization of the KEGG enrichment analysis showed that EDXKD may play a role in the treatment of DM MGD by regulating fat and atherosclerosis and the IL-17 and PPARG signaling pathways (Fig. 2G). To explore the potential mechanism of EDXKD in the treatment of DM MGD, we performed "Herb-Target-Component-Pathway" network information visualization (Fig. 2H). Based on the results of core target screening and KEGG analysis, we speculated that EDXKD may play a therapeutic role in DM MGD by regulating the PPARG signaling pathway.

3.3. Efficacy and potential mechanism of EDXKD in the treatment of DM MGD

Under a posture microscope, the eyelid margins of the DM MGD rats were hypertrophic, hyperemic, and thickened. The fission of the eyelid was narrow, and the shape of the eyelid margin was not smooth. The MG orifice was partially blocked, and lipid deposits were observed in the orifice (Fig. 3A). Corneal fluorescein staining was positive, indicating that MG dysfunction could lead to corneal epithelial damage ($n = 5$) (Fig. 3B). After treatment, the EDXKD group showed a slight reduction in eyelid border hypertrophy compared with that in the DM MGD group. Although the eyelid border remained rounded and obtuse, the corneal fluorescence staining was significantly reduced, and the score was lower in the EDXKD group (Fig. 3C). In addition, when MG function was abnormal, the ocular surface environment changed. Besides corneal injury, the BUT in the DM MGD group was significantly shorter than that in the CON group, and the length of the phenol red thread, which represented the flow of tear secretion, was decreased ($n = 5$). After treatment, the BUT and tear secretion flow in the EDXKD group were significantly higher than those in the DM MGD group, with more significant improvement observed in the middle-dose EDXKD group (Fig. 3D and E).

3.3.1. EDXKD attenuates glucose and lipid metabolism disorders in DM MGD rats

After STZ modeling, the blood glucose level of DM MGD rats was significantly higher than that of normal rats. After 4 weeks of treatment, although there was no significant difference in blood glucose levels between the EDXKD and DM MGD groups, the blood glucose levels in the EDXKD groups tended to decrease ($n = 5$) (Fig. 4A). Simultaneously, rats in the DM MGD group showed disorders of lipid metabolism. After treatment with the EDXKD, TC, TG, and LDL levels decreased significantly, whereas HDL levels increased significantly (Fig. 4B–E).

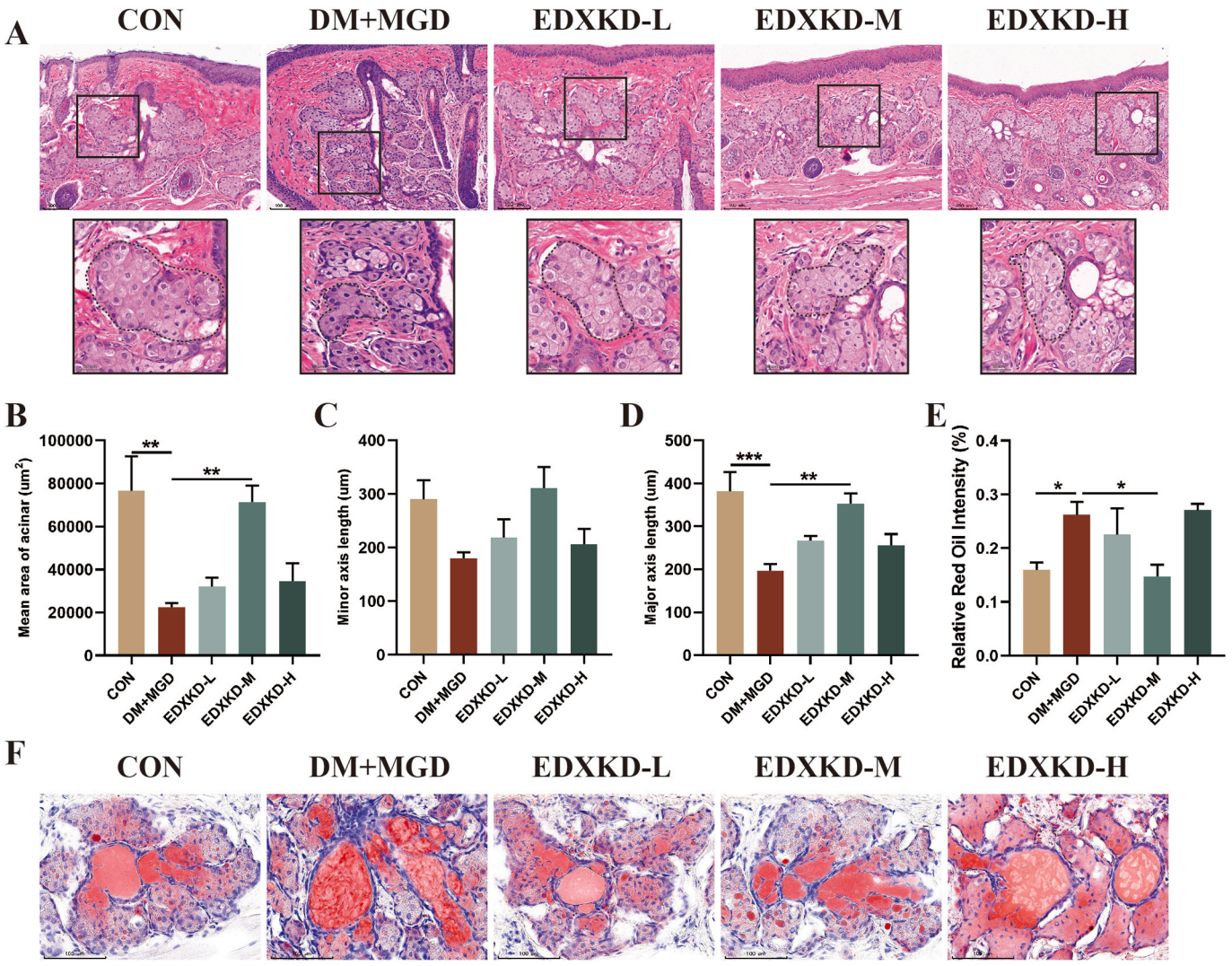

Fig. 5. Histological changes of diabetes mellitus meibomian glands (DM MGs). (A) hematoxylin and eosin (H&E) staining of MGs structure in each group; (B) The mean area, (C) minor axis length, (D) major axis length of acinar in each group. (E) Relative red oil intensity of MGs in each group. (F) Oil Red O staining of MGs structure in each group. (For interpretation of the references to colour in this figure legend, the reader is referred to the Web version of this article.)

3.3.2. *Effect of EDXKD on histology of DM MGs*

H&E staining showed that the acinus around the MG ducts in normal rats was spherical, full, and well-arranged. In the DM MGD group, the ducts were obviously dilated, acini were atrophied, volume shrank, shapes were different, and arrangement was disordered. In the EDXKD-treated group, the acinar was arranged around the ducts, and the acinar volume significantly increased with a slightly regular shape. The measurement of the acinar area and the lengths of the major and minor axes showed that the size of acini was improved (n = 3) (Fig. 5A–D). Oil Red O staining was used to observe lipid accumulation in MG tissues (n = 3). The results showed denser red staining in the atrophied acini and dilated ducts in the DM MGD group. In the treatment group, the red staining of the EDXKD-L and EDXKD-M groups was significantly lower than that of the DM MGD group. Lipids accumulated in the acini and ducts of the EDXKD-L group, whereas most of the EDXKD-M lipids accumulated in the glandular ducts (Fig. 5E–F).

3.3.3. *Lipidomic analysis*

The results of multivariate statistical analysis using principal component analysis (PCA) and orthogonal partial least square discriminant analysis (OPLS-DA) models are shown in Fig. 6A–C. The PCA scores showed obvious separation trends among the control, DM MGD, and EDKXD groups, with significant differences observed among the groups.

We found 183 differentially expressed lipids between diabetic and normal MGs (Supplementary material), of which, 117 were down-regulated, and 66 were upregulated. The main differential lipids were glycerophospholipids (GP), sphingolipids (SP), glycerolipids (GL), fatty acids (FA), and sterol lipids (ST), indicating lipid metabolic disorders in the MGs of DM MGD rats (Fig. 6D and E). To explain the relationship between the effect of T2DM on MGs and the treatment of DM MGD with EDKXD, we assessed the differential lipids among the control, DM MGD, and EDKXD groups, along with the effect of EDKXD on them. Among the differential lipids, triglycerides (TG), ceramides (Cer), and cardiolipins (CL) were most closely associated with the EDXKD-mediated regulation of MG lipid metabolism (Fig. 6F). Notably, 12 lipids showed significant changes post-EDXKD administration, similar to the trend in the control group, reversing the abnormal metabolism of DM MGs (Fig. 6G–Table 3). Typical lipid biomarkers were sphingomyelin (SM), sucrose fatty acid esters (SE), phosphatidylcholine (PC), fatty acyl (FA), bis (monoacylglycerol) phosphate (BMP), and others, with trends shown in Fig. 7A–I. SM (12:1; O2/12:0), SE (24:1; O4/24:4), SE (24:1; O4/21:5), PC (22:6_22:6), BMP (40:8|BMP 18:2_22:6), and SG (28:1; O;Hex) were negatively associated with DM MGD risk, and FA (20:1; O), FA (20:1), and PC (O-19:5_28:77) were positively correlated with DM MGD risk. The most prominent improvement with EDXKD was observed in the

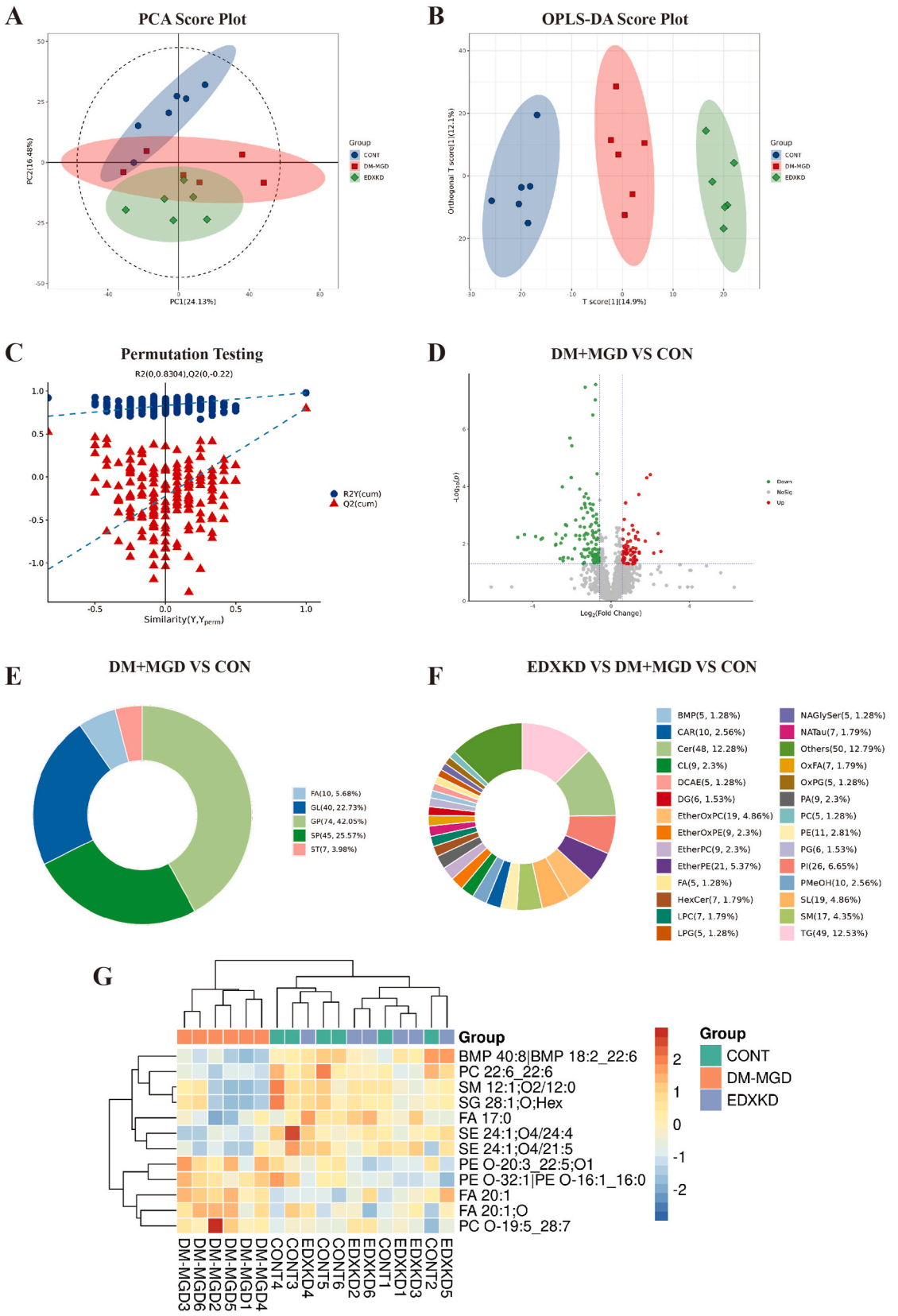

Fig. 6. Regulation of lipids in meibomian glands (MGs) of diabetes mellitus meibomian gland dysfunction (DM MGD) rats by Er-Dong-Xiao-Ke Decoction (EDXKD). (A) principal component analysis (PCA) score plot; (B) orthogonal partial least square discriminant analysis (OPLS-DA) score plot (EDXKD vs. DM MGD vs. CON); (C) permutation testing diagram; (D) volcano (DM MGD vs. CON), red dots are upregulated metabolites and green dots are down-regulated metabolites; (E) statistical ring diagram of differential lipid classification (DM MGD vs. CON); (F) subclass statistical ring diagram of differential lipid molecules (EDXKD vs. DM MGD vs. CON); (G) cluster heatmap of potential biomarkers for each group. (For interpretation of the references to colour in this figure legend, the reader is referred to the Web version of this article.)

Table 3
Identified prototype components of EDXKD in DM MGs based on LC-MS/MS.

NO.	Metabolite name	RT(min)	P-value	Average (m/z)	Reference (m/z)	Formula	Ontology	LipidMapsClass
1	FA 17:0	24.655	0.014677589	269.24832	269.2486	C17H34O2	FA	FA
2	PC 22:6_22:6	18.321	0.000944146	922.55951	922.56042	C52H80NO8P	PC	GP
3	FA 20:1	12.639	0.002275543	309.28024	309.27991	C20H38O2	FA	FA
4	SM 12:1; O2/12:0	17.722	0.014660764	607.40753	607.4093	C29H59N2O6P	SM	SP
5	BMP 40:8|BMP 18:2_22:6	16.865	0.001402482	836.54425	836.54358	C46H75O10P	BMP	GP
6	SE 24:1; O4/24:4	21.247	0.003887613	733.57916	733.57758	C48H78O5	DCAE	ST
7	SG 28:1; O;Hex	17.691	0.029603688	607.42175	607.42151	C34H58O6	SHex	ST
8	PE O-20:3_22:5; O1	23.232	0.002195031	816.55511	816.55487	C47H80NO8P	EtherOxPE	GP
9	FA 20:1; O	3.709	0.027548973	325.27457	325.27481	C20H38O3	OxFA	FA
10	PC O-19:5_28:7	22.231	0.013896504	906.63458	906.63708	C55H88NO7P	EtherPC	GP
11	PE O-32:1|PE O-16:1_16:0	23.09	0.000669696	674.51031	674.513	C37H74NO7P	EtherPE	GP
12	SE 24:1; O4/21:5	20.499	0.038085736	689.51819	689.51501	C45H70O5	DCAE	ST

glycerophospholipid metabolic pathway (Fig. 7J).

3.3.4. EDXKD increases the expression of PPARG in DM MGs

Immunofluorescence results showed that the fluorescence intensity of PPARG in DM MGs decreased, and the localization of PPARG in some acinar cells disappeared. However, PPARG expression in the EDXKD-treated group increased to varying degrees (n = 3) (Fig. 8A and B). RT-qPCR and western blotting further confirmed that the expression of PPARG in the DM MGD group decreased, whereas EDXKD intervention upregulated the expression of PPARG (n = 3) (Fig. 8C and D).

3.3.5. Lipid metabolism disorder in DM MGD and the UCP2/AMPK signal pathway

To further explore the mechanism of lipid metabolism disorders in DM MGD, we analyzed the genes and proteins encoding lipid metabolism-related factors in the MGs of DM MGD rats. A significant decrease was observed in the gene expression of MTTP and APOB in the MG tissues of the DM MGD group, compared with those in the normal group (Fig. 9A and B). Additionally, the expression of the fatty acid transporter CD36 and p-ACC decreased significantly (n = 3) (Fig. 9C–E). EDXKD increased the expression of CD36, MTTP, APOB, and p-ACC in DM MGs.

Further, we observed an increase in the expression of UCP2 and a decrease in the expression of p-AMPK in the DM MGs. However, the expression level of UCP2 in the EDKXD group was significantly lower than that in the DM MGD group, and the phosphorylation level of AMPK was increased (n = 3) (Fig. 9F–H).

3.4. EDXKD treats DM MGD by regulating the PPARG signal pathway

3.4.1. PPARG is the key target of EDXKD in the treatment of DM MGD

To further verify the effect of EDXKD on PPARG, we confirmed by immunofluorescence that the expression of PPARG in the T0070907 group was lower than that in the DM MGD group, and the localization deletion was more obvious (n = 3). Compared with the T0070907 group, PPARG in the EDXKD + T0070907 group increased significantly (Fig. 10A and B). Western blotting and RT-qPCR confirmed that after EDXKD treatment, the expression of PPARG in the EDXKD group was significantly higher than that in the DM MGD group, and the expression of PPARG in the EDXKD + T0070907 group was higher than that in the T0070907 group (n = 3) (Fig. 10C and D).

After inhibiting the expression of PPARG in the DM MGD group, glucose and lipid metabolism disorder in the T0070907 group was more severe than that in the DM MGD group, and treatment with EDXKD improved the levels of blood glucose and lipids (n = 5) (Fig. 11A–E). Simultaneously, the eyelid margins of the T0070907 group were as thick and blunt as those of the DM MGD group, and the orifices of the glandular ducts were occluded. However, dry eye symptoms in the T0070907 group were more severe than those in the DM MGD group (Fig. 11I and J). Compared with the T0070907 group, BUT and PRT levels increased, and the FL score decreased in the EDXKD + T0070907 group. Although not statistically significant, all showed an improving trend (Fig. 11F–H).

H&E staining showed that when PPARG expression was inhibited, the arrangement of acinar cells in the MGs in the T0070907 group was more disordered than that in the DM MGD group. The shape was smaller and deformed, and the glandular tubes were not only dilated but also arranged more sparsely, with thickened walls of the glandular tubes (n = 3). After treatment, there were more acini around the glandular duct, and the acini in the EDXKD + T0070907 group were rounder than those in the T0070907 group (Fig. 11K). Calculations of the acinar area and the major axis and minor axis lengths showed that EDXKD can effectively improve the shape of acinars with T0070907 (Fig. 11L-N). Compared with the DM MGD group, the atrophic acini of MGs in the T0070907 group were more severe and had denser red staining. Additionally, substantial lipid accumulation was observed in the dilated ducts, whereas red staining was alleviated in some acini of the EDXKD + T0070907 group (n = 3) (Fig. 11O-P).

3.4.2. EDXKD activates the PPARG signal pathway to regulate lipid metabolism of DM MGD

We used the PPARG inhibitor T0070907 to evaluate whether EDXKD could regulate lipids and improve DM MGD by activating the PPARG/UCP2/AMPK signaling pathway. The expression levels of proteins and genes in the UCP2/AMPK signaling pathway were detected by western blotting and RT-qPCR (n = 3). After T0070907 inhibited the expression of PPARG, compared with the DM MGD group, the expression of UCP2 increased, and the expression of p-AMPK, ACC, CD36, APOB, and MTTP decreased. However, treatment with EDXKD restored the PPARG-mediated low expression of UCP2 and upregulated the expression of p-AMPK, ACC, CD36, APOB, and MTTP (Fig. 12A–H).

4. Discussion

Approximately half of patients with diabetes have dry eyes, and the prevalence of MGD in patients with diabetes is approximately 39.9% (Hom and De Land, 2006). Hyperglycemia affects the normal differentiation of MG acinar cells, resulting in duct obstruction, lipid accumulation, and MGD (Guo et al., 2022). Lipid deposition is the main pathological basis for T2DM and MGD. Traditionally, DM MGD is characterized by “blood stasis,” with its main pathogenesis involving yin deficiency and excessive heat, resulting in fluid deficiency. EDXKD regulates lipids by “nourishing yin, clearing heat, and removing blood stasis.” LC-MS/MS analysis showed that the main chemical constituents of EDXKD were isoflavone glycosides, original berberine, and terpenoids. Combined with the network analysis, we found that geranylacetone, magnoflorine, jatrorrhizine, quercetin, scoparone, berberine, and palmatin are the effective components of EDXKD and have the largest degree of freedom, involving a wide range of targets and applications. Magnoflorine has various pharmacological effects such as the inhibition of α-glucosidase, promotion of insulin release to improve glucose levels in diabetic rats and significant inhibition of lipogenesis in

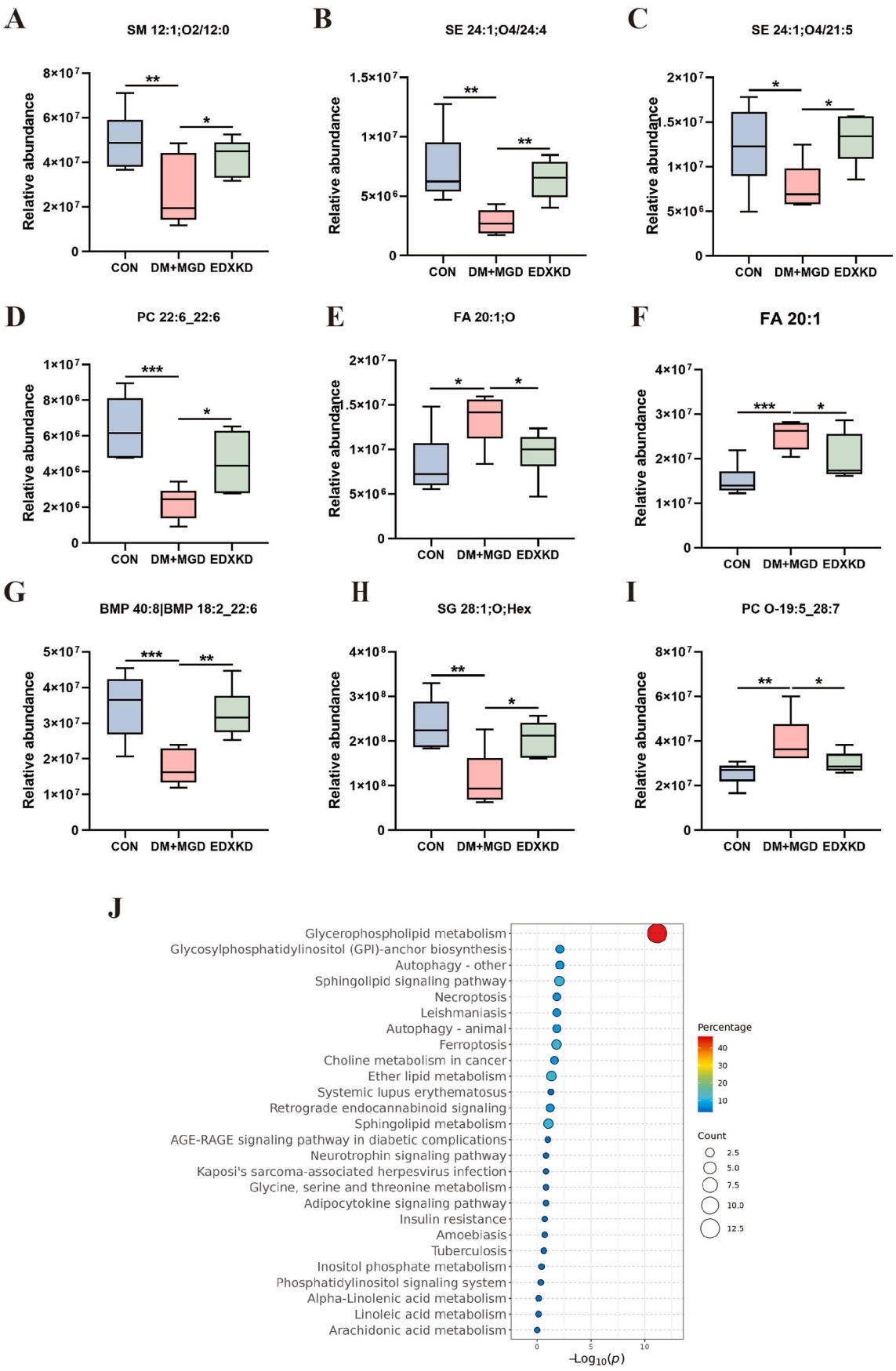

Fig. 7. Er-Dong-Xiao-Ke Decoction (EDXKD) ameliorates lipid metabolism disorders in meibomian glands (MGs) of diabetes mellitus meibomian gland dysfunction (DM MGD) rats. (A–I) comparative analysis of relative content of lipid biomarkers; (J) Kyoto Encyclopedia of Genes and Genomes (KEGG) enrichment map of differential lipids.

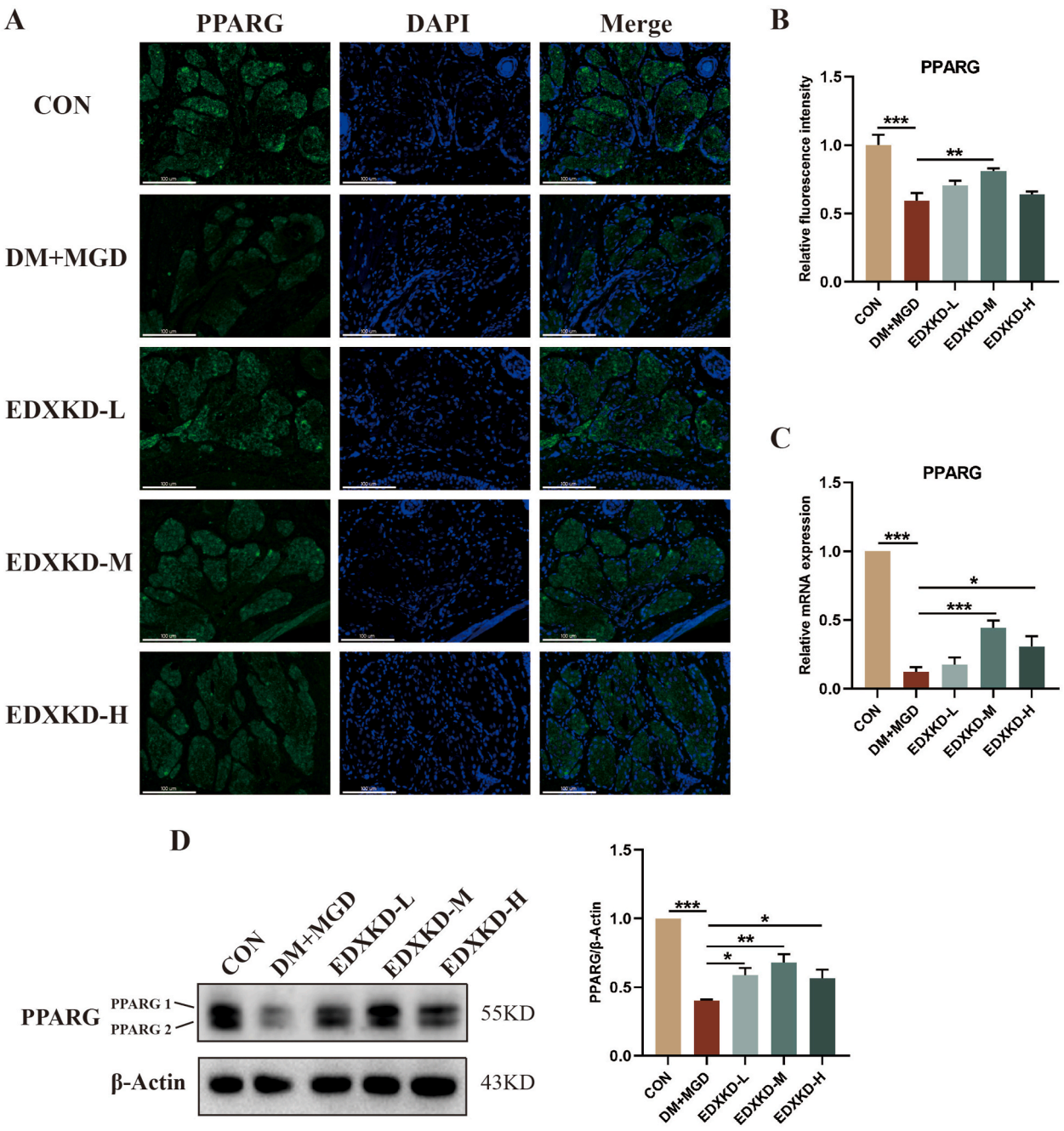

Fig. 8. Er-Dong-Xiao-Ke Decoction (EDXKD) regulates the expression of PPARG in diabetes mellitus meibomian glands (DM MGs). (A) immunofluorescence staining of PPARG in the MGs of each group; (B) relative fluorescence intensity of PPARG; (C) relative mRNA expression of PPARG; (D) western blotting analysis of PPARG in each group.

a dose-dependent manner, with good anti-diabetic and anti-obesity activity (Okon et al., 2020). Jatrorrhizine is one of the major bioactive protoberberine alkaloids found in Huanglian, which has hypoglycemic and hypolipidemic potential and improves diabetes and obesity by reducing ER stress and oxidative stress (Zhou et al., 2022). Quercetin can act as an agonist or modulator of PPARG and has a potential regulatory effect on T2DM and dyslipidemia (Villarroel-Vicente et al., 2021). Scoparone improve the blood lipids and vascular morphology of rabbits with hyperlipemia and diabetes (Huang et al., 1993). Berberine is a well-known chemical component for the treatment of T2DM; in mice models, it promoted the PPARG-regulated FGF21/GLUT2 pathway, thereby regulating insulin sensitivity and glycolipid homeostasis (Chen et al., 2023). Palmatin, as a potential natural cholesterol-lowering agent, can significantly reduce the level of blood lipids in hyperlipemia hamsters and exert its lipid-lowering effect (Ning et al., 2015; Nwabueze et al., 2022). These therapeutic characteristics make EDXKD advantageous for the treatment of dyslipidemia of DM MGD.

In this study, we observed that EDXKD treats DM MGD by regulating lipid metabolism. The pathological results showed that EDXKD reduced lipid accumulation in the acini and ducts of DM MGs, improved acinar morphology, and increased acinar density. With the reduction in MG lipid accumulation and the recovery of systemic blood lipid levels, the ocular surface indices of diabetic rats improved. To analyze the lipids in diabetic MGs, LC-MS/MS was conducted and showed that GP, GL, and SP were the main effects of EDXKD on DM MGD. In further analysis of lipid subclasses, CL, TG, and Cer were significantly different lipid

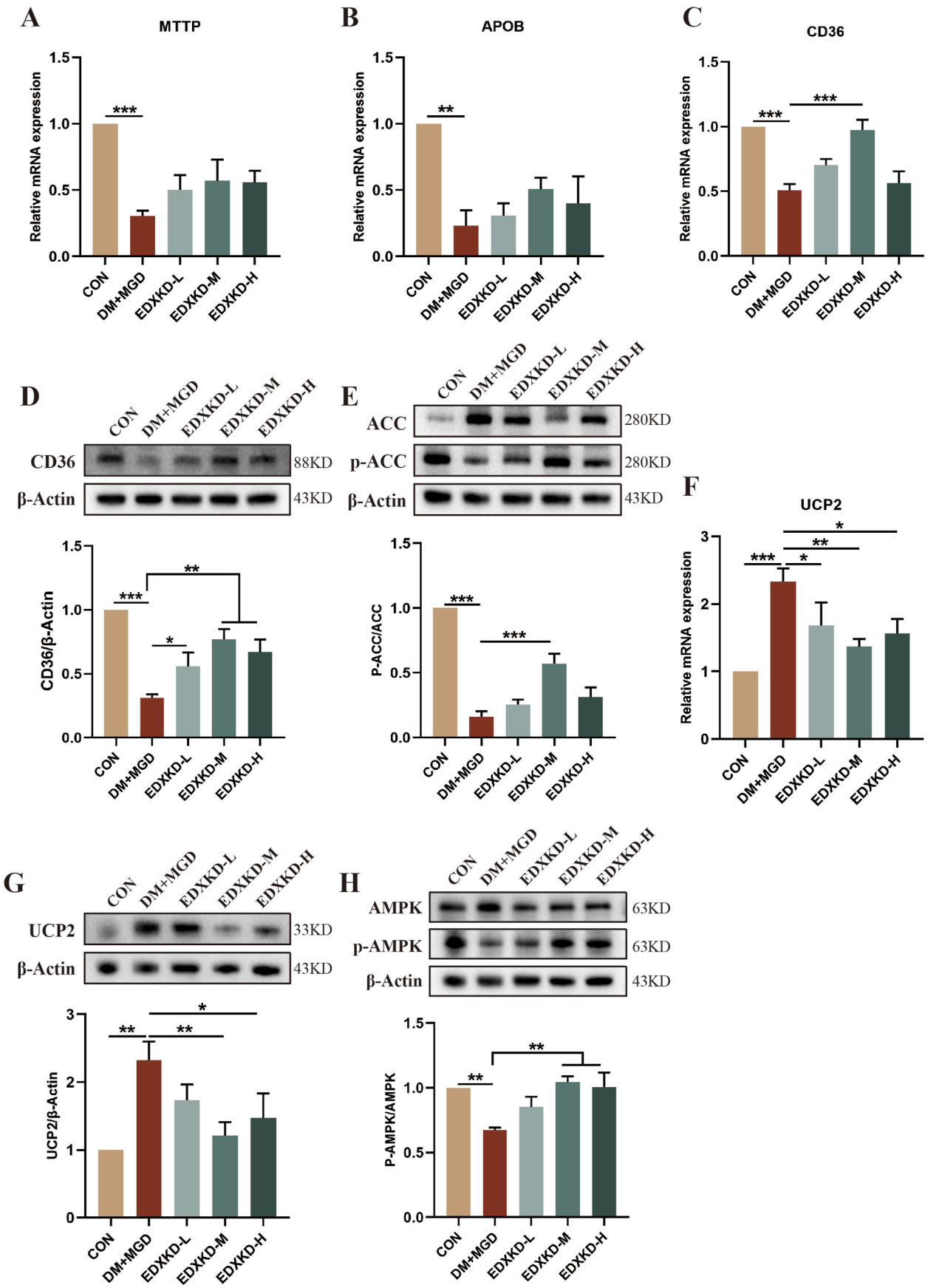

Fig. 9. Er-Dong-Xiao-Ke Decoction (EDXKD) improves the expression of lipid metabolism-related factors in diabetes mellitus meibomian gland dysfunction (DM MGD) rats. Relative mRNA expression of lipid metabolism-related factor (A) MTTP; (B) APOB; (C) CD36 in meibomian glands (MGs); and western blotting results of

(D) CD36 and (E) ACC in each group; (F, G) relative expression of energy metabolism-related factor UCP2 in MGs; and (H) western blotting result of AMPK in each group.

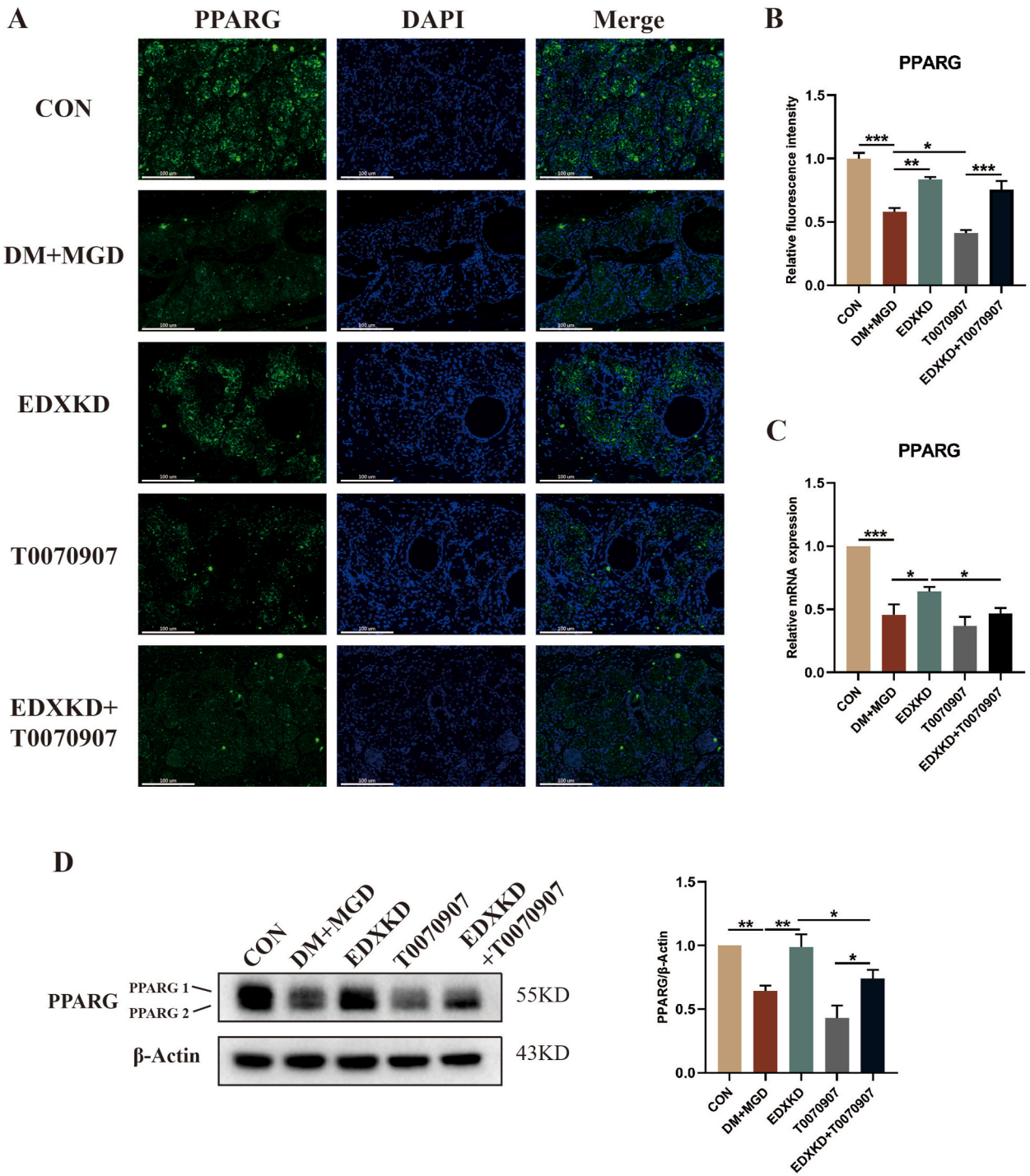

Fig. 10. PPARG is the target for Er-Dong-Xiao-Ke Decoction (EDXKD). (A) immunofluorescence staining of PPARG in meibomian gland (MG) tissues of each group; (B) relative fluorescence intensity of PPARG; (C) relative mRNA expression of PPARG; (D) western blotting analysis of PPARG in each group.

molecules. We further studied the possible markers of EDXKD in the treatment of DM MGD and finally identified 12 kinds of lipid molecules, mainly concentrated in PC, BMP, SE, and other lipids, most of which belong to GPs. The intervention of EDXKD could reverse the expression of these lipids. SM, SE, PC, BMP, and SG were negatively associated, while FA was positively correlated with DM MGD risk. There was a significant difference in PC in our experimental results. PC is a key by-product of the GP metabolic pathway, and lower PC is a risk factor for metabolic diseases such as obesity and diabetes (Park et al., 2015). Increasing exogenous PC can reduce chronic inflammation and improve lipid metabolic disorders (Fang et al., 2022). EPA-rich PC can upregulate the expression of PPARG lipid metabolism target genes and improve insulin resistance and abnormal lipid accumulation (Tian et al., 2020). Combined with the pathways identified by KEGG enrichment and the

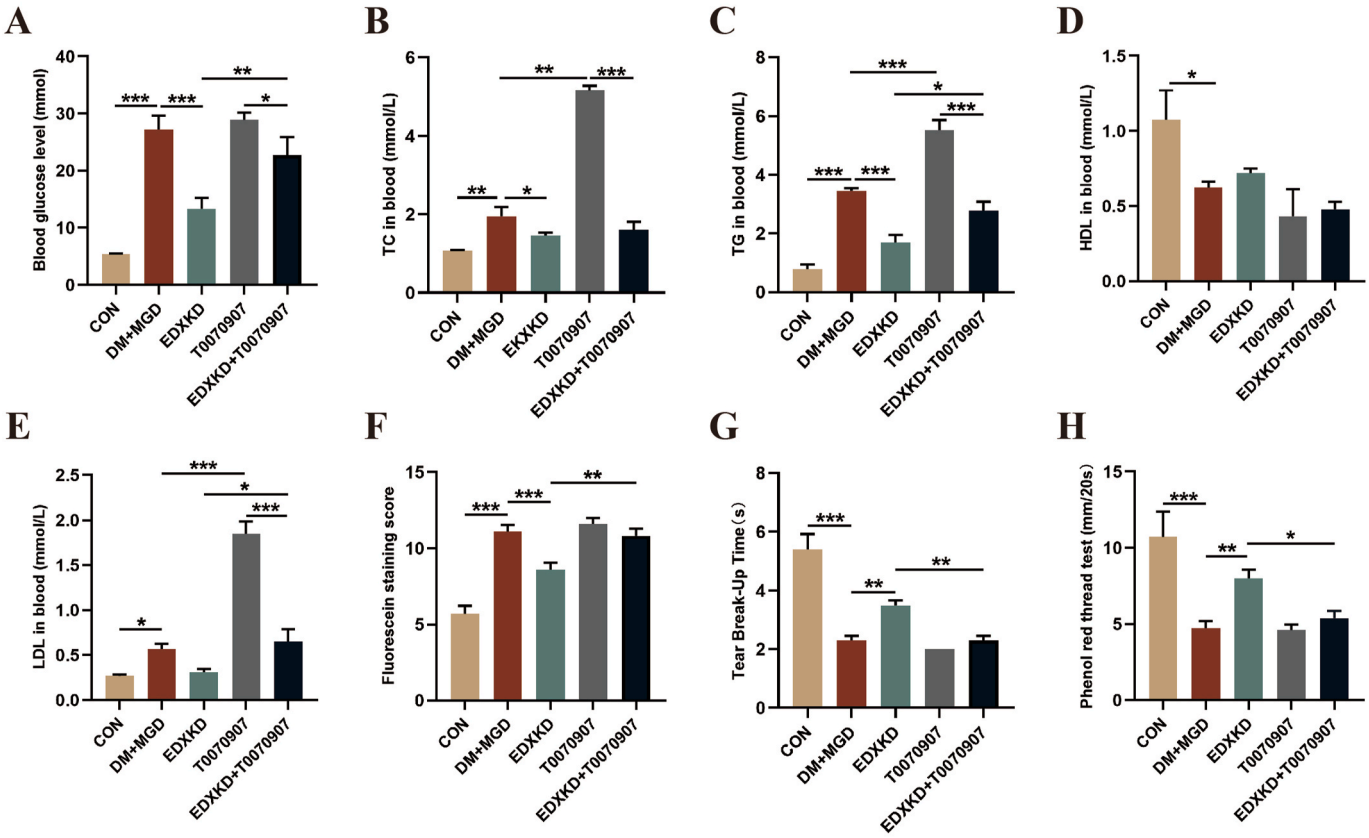

Fig. 11. Er-Dong-Xiao-Ke Decoction (EDXKD) improves glycolipid metabolism and ocular surface function in diabetes mellitus meibomian gland dysfunction (DM MGD) rats by modulating PPARG. (A–E) blood glucose and lipid levels; (F–H) FL, BUT, and PRT in each group; (I) observation of the eyelid performance of each group; (J) fluorescein staining images of the cornea in each group; (K) H&E staining of MGs structure in each group; (L–N) The mean area, (C)minor axis length, and (D)major axis length of acinar in each group; (O–P) Oil Red O staining and intensity of MGs structure in each group. (For interpretation of the references to colour in this figure legend, the reader is referred to the Web version of this article.)

above discussion, GP metabolism may be an important pathway by which EDXKD improves DM MGD. In addition, SP metabolism is also a pathway closely related to DM MGD. The accumulation of SM and Cer is closely related to T2DM and MGD. The content of SM increases with the increase of cholesterol content, and SM can be hydrolyzed and activated by sphingomyelinase to form Cer (Galadari et al., 2013; Kostara et al., 2021). The content of Cer in MGs of DM mice increased significantly, and the abnormal Cer metabolism caused cell cycle arrest and destroyed the lipid balance in DM mice (Wang et al., 2021). Our results further support that these metabolites can be used as biomarkers to detect DM MGD. However, the relationship between some lipid molecules, such as SE and SG, and diabetes and MGD has not been studied, which may be an opportunity to identify DM MGD biomarkers in the future.

Liquid LC-MS and network pharmacological analyses revealed a significant relationship between PPARG and EDXKD in the treatment of DM MGD. PPARG plays a crucial role in regulating the dynamic balance between lipid and glucose levels. PPARG inactivation leads to metabolic abnormalities such as diabetes, insulin resistance, and dyslipidemia (Ahmadian et al., 2013). Therefore, the PPARG signaling pathway plays a key role in regulating the abnormal lipid metabolism associated with diabetes. Activating PPARG can promote the downstream signal pathway of FGF21 to reduce lipid accumulation, alleviate inflammation and insulin resistance, and improve the damage caused by hyperglycemia and lipotoxicity (Chen et al., 2023). Furthermore, stimulating PPARG expression can promote adiponectin signal transduction, thereby reducing lipid accumulation and mitochondrial dysfunction in patients with diabetes, thus preventing diabetic cardiomyopathy (Zhang et al., 2023). Lipid metabolism disorders in MGD are related to a decrease in the expression of PPARG, a lipid-sensitive nuclear receptor (Jester et al., 2016). Similar to previous reports, the immunofluorescence results showed that the expression of PPARG in the MGs of rats with DM was significantly decreased and that EDXKD intervention promoted the expression of PPARG. Additionally, western blotting and RT-qPCR experiments confirmed that EDXKD improved the expression of PPARG, lipid synthesis (ACC), and lipid transport (CD36, APOB, and MTTP) in MGs. Both MTTP and APOB belong to the lipid transfer protein family, which can bind to and transfer various lipid molecules to promote lipid transport (Hooper et al., 2015). CD36 is a single-stranded transmembrane surface glycoprotein located on the membrane of acinar cells near the MG ducts (Zheng et al., 2016). As a classical downstream factor of PPARG, CD36 can promote the uptake of long-chain fatty acids, activate fat degradation, and bind to oxidized lipoproteins to coordinate lipid metabolism (Pan et al., 2023). ACC is a key enzyme in fatty acid synthesis that can be activated by AMPK phosphorylation to inhibit cholesterol and fatty acid synthesis (Guo et al., 2023). Considering the stable performance of the medium-dose EDXKD group in the experiment, we suggest that the medium dose may be the best when administering EDXKD. T0070907 is an effective and selective PPARG antagonist. We used a stable medium-dose EDXKD and T0070907 to further evaluate the effects of EDXKD on DM MGD. After T0070907 suppressed the expression of PPARG, the expression levels of ACC, CD36, APOB, and MTTP were lower than those in the DM MGD group. Although these levels increased after treatment with EDXKD, they were still significantly lower than those observed in the EDXKD group. The pathological results showed that the lack of PPARG aggravated lipid deposition in the MGs of DM MGD rats. We concluded

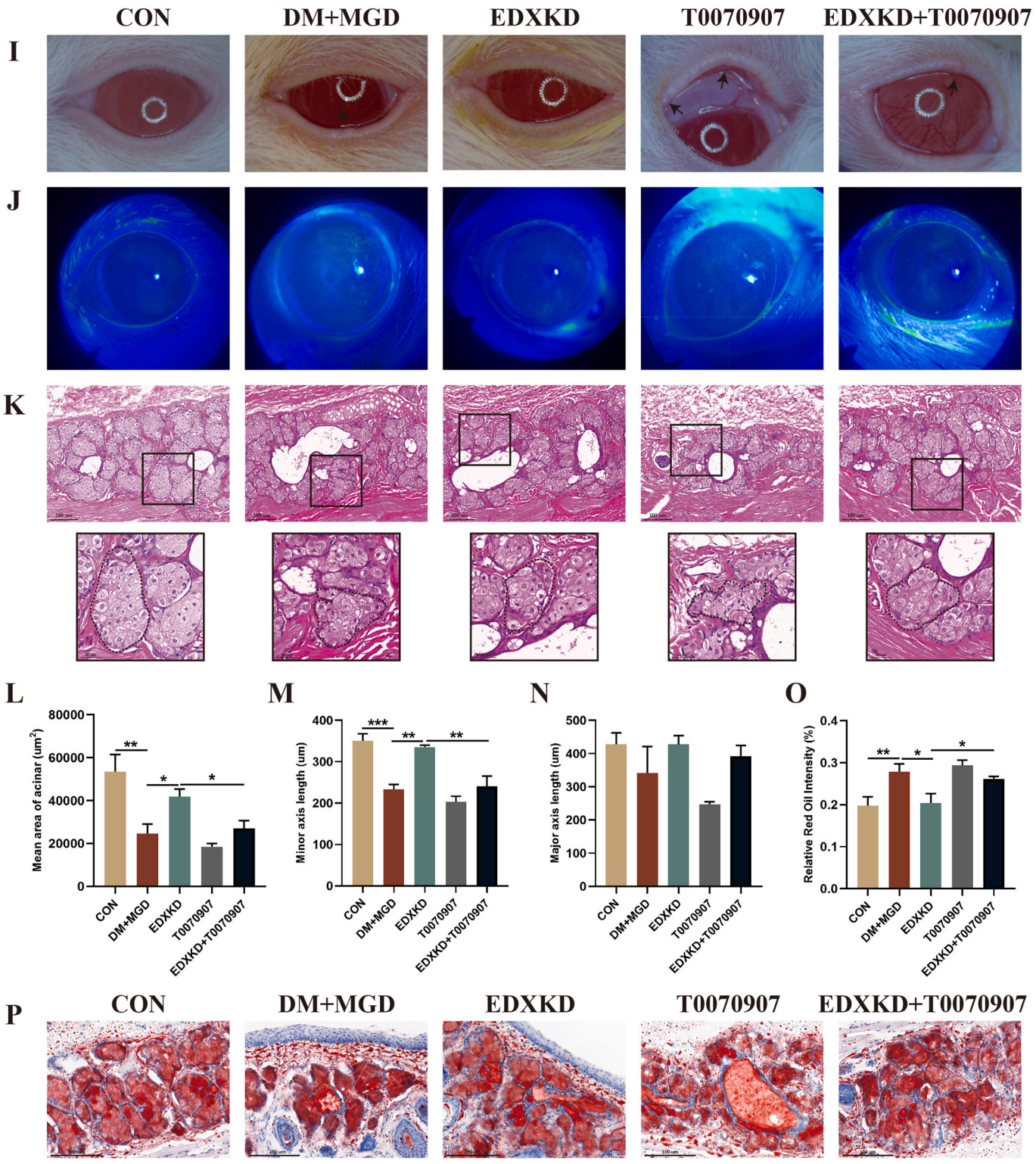

Fig. 11. (*continued*).

that PPARG is the key to the pathogenesis of DM MGD and that EDXKD can improve DM MGD by activating PPARG targets, which inhibit lipid synthesis, promote lipid transport in DM MGs, and reduce lipid deposition in acini and ducts.

UCP2, a member of the UCP family of mitochondria, uncouples the oxidative and phosphorylation processes of the respiratory chain by eliminating inner mitochondrial membrane proton gradients. Lipid peroxidation of polyunsaturated fatty acids and hydrogen peroxidation products can activate UCP2 to produce tricarboxylic acid cycle intermediates, inhibit glucose metabolism, increase mitochondrial fatty acid oxidation, and reduce adenosine triphosphate (ATP) synthesis to downregulate reactive oxygen species (ROS) (Diano and Horvath, 2012). AMPK is a metabolic receptor that varies with the concentrations of adenosine monophosphate (AMP), adenosine diphosphate (ADP), and ATP. A high AMP/ATP or ADP/ATP ratio can promote the phosphorylation and utilization of lipids in cells (Herzig and Shaw, 2018). The

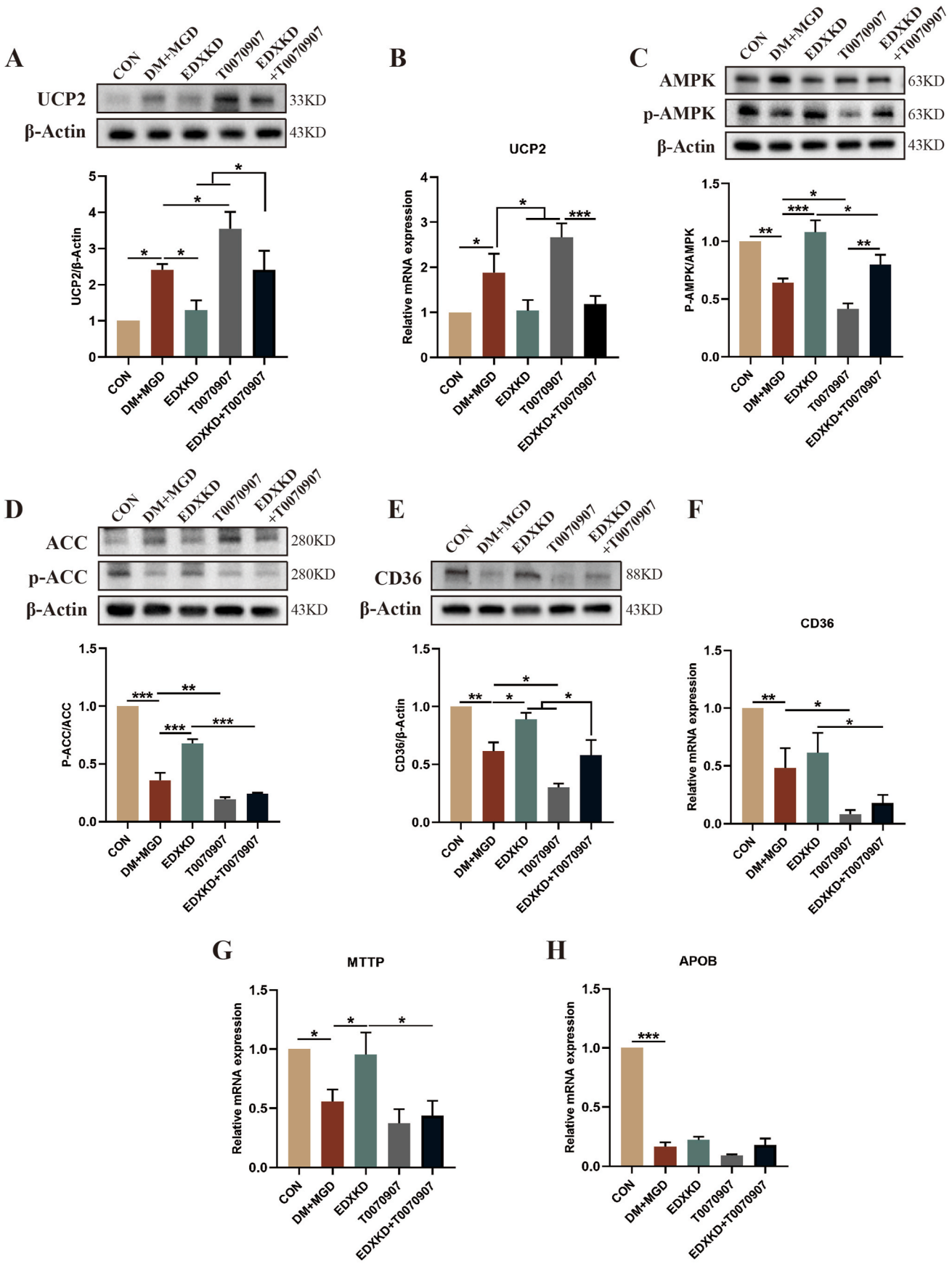

Fig. 12. Er-Dong-Xiao-Ke Decoction (EDXKD) regulates lipid metabolism by PPARG-mediated UCP2/AMPK signaling network; (A–B) expression levels of UCP2; (C) AMPK; (D) ACC; (E–F) CD36; (G) MTTP; and (H) APOB in the meibomian glands (MGs) of each group.

UCP2/AMPK/ACC signaling pathway regulates lipid accumulation in hepatocytes (Li et al., 2023b). UCP2 gene knockout increased the AMP/ATP ratio and AMPK phosphorylation in adipocytes, upregulated ACC expression, and promoted fatty acid oxidation (Yu et al., 2019). Combined with our experimental results, the high expression of UCP2 in DM MGD inhibited the activation of AMPK, hindered fatty acid oxidation of ACC, and aggravated lipid accumulation in MGs. PPARG inactivation hinders lipid synthesis and transport in cells. Lipid deposition induces oxidative stress-induced injury and accelerates lipid peroxide formation. Fatty acids and hydrogen peroxidation products of lipid peroxidation activate UCP2 (Berbée et al., 2017). Overexpression of UCP2 inhibits the AMPK/ACC signaling pathway, which affects fatty acid oxidation and aggravates lipid metabolism disorders in MGs. EDXKD upregulates PPARG expression and reduces oxidative stress and lipid peroxidation, resulting in a decrease in the expression of UCP2. The decrease in UCP2 levels promotes the activation of the AMPK/ACC signaling pathway of lipid oxidation and improves lipid metabolism. When EDXKD affects the UCP2/AMPK signaling network, changes in the AMP/ATP ratio and lipid oxidation levels need to be further verified.

Our research shows that the mechanism by which EDXKD improves DM MGD may be associated with the regulation of lipid metabolism by the PPARG-mediated UCP2/AMPK signaling network, which provides scientific support for the development of clinical plans and strategies for the treatment of T2DM MGD using EDXKD. However, this study had some limitations. First, three different doses were selected to explore the efficacy of EDXKD, and no dose dependence was found. We speculate that there might be an off-target effect in the high-dose group because of the multi-target character of the compound preparation (Zhao et al., 2020). Moreover, we examined the liver and kidney functions of the three dose groups and found that the liver and kidney functions of the high-dose group may reflect some damage and toxic reactions, which led to no dose dependence (Supplementary Material). Therefore, it is very important to reveal the pharmacodynamics and pharmacokinetics of EDXKD through further research, and we will explore the effective and safe dose range of EDXKD in more detail and more comprehensively in follow-up studies. The compound contains a variety of chemical components; however, what makes EDXKD more effective remains unclear. In the next step, the active ingredients that have not been studied are the focus of the study. Additionally, our study only explored the regulation of lipid metabolism by the PPARG-mediated UCP2/AMPK signaling network. Specific changes in energy metabolism need to be further studied.

5. Conclusion

In conclusion, this study explored, for the first time, the mechanism of EDXKD in treating T2DM with MGD by reducing lipid accumulation through a PPARG-mediated UCP2/AMPK signaling network. Future studies will focus on identifying the main active components of EDXKD and demonstrating their corresponding lipid-regulating effects.

CRediT authorship contribution statement

Li Shi: Writing – original draft, Methodology, Investigation, Data curation. **Liu-Jiao Li:** Methodology, Investigation, Data curation. **Xin-Yi Sun:** Methodology, Investigation. **Yi-Ying Chen:** Validation, Methodology, Conceptualization. **Dan Luo:** Data curation. **Lu-Ping He:** Validation, Methodology. **Hui-Jie Ji:** Validation, Methodology. **Wei-Ping Gao:** Writing – review & editing, Resources, Conceptualization. **Hu-Xing Shen:** Writing – review & editing, Resources, Conceptualization.

Declaration of competing interest

The authors declare that they have no known competing financial interests or personal relationships that could have appeared to influence the work reported in this paper.

Data availability

Data will be made available on request.

Acknowledgments

This study was supported by the National Natural Science Foundation of China (No. 82074526; No. 82305320) and the Cadre Health Research Project of the Jiangsu Provincial Health Commission (No. BJ23012). We thank FigDraw for providing the graphical abstract. Besides, we are grateful to Shanghai Bioprofile Technology Co., Ltd. For technical support in massspectroscopy.

Appendix A. Supplementary data

Supplementary data to this article can be found online at https://doi.org/10.1016/j.jep.2024.118484.

References

Ahmadian, M., Suh, J.M., Hah, N., Liddle, C., Atkins, A.R., Downes, M., Evans, R.M., 2013. PPARγ signaling and metabolism: the good, the bad and the future. Nat. Med. 19 (5), 557–566. https://doi.org/10.1038/nm.3159.

Almugadam, B.S., Yang, P., Tang, L., 2021. Analysis of jejunum microbiota of HFD/STZ diabetic rats. Biomed. Pharmacother. 138, 111094 https://doi.org/10.1016/j.biopha.2020.111094.

Berbée, J.F.P., Mol, I.M., Milne, G.L., Pollock, E., Hoeke, G., Lütjohann, D., Monaco, C., Rensen, P.C.N., van der Ploeg, L.H.T., Shchepinov, M.S., 2017. Deuterium-reinforced polyunsaturated fatty acids protect against atherosclerosis by lowering lipid peroxidation and hypercholesterolemia. Atherosclerosis 264, 100–107. https://doi.org/10.1016/j.atherosclerosis.2017.06.916.

Berger, J., Moller, D.E., 2002. The mechanisms of action of PPARs. Annu. Rev. Med. 53, 409–435. https://doi.org/10.1146/annurev.med.53.082901.104018.

Blackie, C.A., Carlson, A.N., Korb, D.R., 2015. Treatment for meibomian gland dysfunction and dry eye symptoms with a single-dose vectored thermal pulsation: a review. Curr. Opin. Ophthalmol. 26 (4), 306–313, 10.1097/icu.0000000000000165.

Chen, Y., Li, Q., Zhao, S., Sun, L., Yin, Z., Wang, X., Li, X., Iwakiri, Y., Han, J., Duan, Y., 2023. Berberine protects mice against type 2 diabetes by promoting PPARγ-FGF21-GLUT2-regulated insulin sensitivity and glucose/lipid homeostasis. Biochem. Pharmacol. 218, 115928 https://doi.org/10.1016/j.bcp.2023.115928.

Chhadva, P., Goldhardt, R., Galor, A., 2017. Meibomian gland disease: the role of gland dysfunction in dry eye disease. Ophthalmology 124 (11s), S20–s26. https://doi.org/10.1016/j.ophtha.2017.05.031.

Cote, S., Zhang, A.C., Ahmadzai, V., Maleken, A., Li, C., Oppedisano, J., Nair, K., Busija, L., Downie, L.E., 2020. Intense pulsed light (IPL) therapy for the treatment of meibomian gland dysfunction. Cochrane Database Syst. Rev. 3 (3), Cd013559 https://doi.org/10.1002/14651858.Cd013559.

Diano, S., Horvath, T.L., 2012. Mitochondrial uncoupling protein 2 (UCP2) in glucose and lipid metabolism. Trends Mol. Med. 18 (1), 52–58. https://doi.org/10.1016/j.molmed.2011.08.003.

Fakih, D., Zhao, Z., Nicolle, P., Reboussin, E., Joubert, F., Luzu, J., Labbé, A., Rostène, W., Baudouin, C., Mélik Parsadaniantz, S., Réaux-Le Goazigo, A., 2019. Chronic dry eye induced corneal hypersensitivity, neuroinflammatory responses, and synaptic plasticity in the mouse trigeminal brainstem. J. Neuroinflammation 16 (1), 268. https://doi.org/10.1186/s12974-019-1656-4.

Fan, F., Li, X., Li, K., Jia, Z., 2021. To Find Out the relationship between levels of glycosylated hemoglobin with meibomian gland dysfunction in patients with type 2 diabetes. Therapeut. Clin. Risk Manag. 17, 797–807. https://doi.org/10.2147/tcrm.S324423.

Fang, X., Miao, R., Wei, J., Wu, H., Tian, J., 2022. Advances in multi-omics study of biomarkers of glycolipid metabolism disorder. Comput. Struct. Biotechnol. J. 20, 5935–5951. https://doi.org/10.1016/j.csbj.2022.10.030.

Furman, B.L., 2021. Streptozotocin-induced diabetic models in mice and rats. Curr Protoc 1 (4), e78. https://doi.org/10.1002/cpz1.78.

Galadari, S., Rahman, A., Pallichankandy, S., Galadari, A., Thayyullathil, F., 2013. Role of ceramide in diabetes mellitus: evidence and mechanisms. Lipids Health Dis. 12, 98. https://doi.org/10.1186/1476-511x-12-98.

Guo, T., Yan, W., Cui, X., Liu, N., Wei, X., Sun, Y., Fan, K., Liu, J., Zhu, Y., Wang, Z., Zhang, Y., Chen, L., 2023. Liraglutide attenuates type 2 diabetes mellitus-associated non-alcoholic fatty liver disease by activating AMPK/ACC signaling and inhibiting ferroptosis. Mol. Med. 29 (1), 132. https://doi.org/10.1186/s10020-023-00721-7.

Guo, Y., Zhang, H., Zhao, Z., Luo, X., Zhang, M., Bu, J., Liang, M., Wu, H., Yu, J., He, H., Zong, R., Chen, Y., Liu, Z., Li, W., 2022. Hyperglycemia induces meibomian gland dysfunction. Invest. Ophthalmol. Vis. Sci. 63 (1), 30. https://doi.org/10.1167/iovs.63.1.30.

Habtemichael, E.N., Li, D.T., Camporez, J.P., Westergaard, X.O., Sales, C.I., Liu, X., López-Giráldez, F., DeVries, S.G., Li, H., Ruiz, D.M., Wang, K.Y., Sayal, B.S., González Zapata, S., Dann, P., Brown, S.N., Hirabara, S., Vatner, D.F., Goedeke, L., Philbrick, W., Shulman, G.I., Bogan, J.S., 2021. Insulin-stimulated endoproteolytic

TUG cleavage links energy expenditure with glucose uptake. Nat. Metab. 3 (3), 378–393. https://doi.org/10.1038/s42255-021-00359-x.
Herzig, S., Shaw, R.J., 2018. AMPK: guardian of metabolism and mitochondrial homeostasis. Nat. Rev. Mol. Cell Biol. 19 (2), 121–135. https://doi.org/10.1038/nrm.2017.95.
Hom, M., De Land, P., 2006. Self-reported dry eyes and diabetic history. Optometry 77 (11), 554–558. https://doi.org/10.1016/j.optm.2006.08.002.
Hooper, A.J., Burnett, J.R., Watts, G.F., 2015. Contemporary aspects of the biology and therapeutic regulation of the microsomal triglyceride transfer protein. Circ. Res. 116 (1), 193–205. https://doi.org/10.1161/circresaha.116.304637.
Huang, H.C., Weng, Y.I., Lee, C.R., Jan, T.R., Chen, Y.L., Lee, Y.T., 1993. Protection by scoparone against the alterations of plasma lipoproteins, vascular morphology and vascular reactivity in hyperlipidaemic diabetic rabbit. Br. J. Pharmacol. 110 (4), 1508–1514. https://doi.org/10.1111/j.1476-5381.1993.tb13993.x.
Jester, J.V., Nicolaides, N., Smith, R.E., 1981. Meibomian gland studies: histologic and ultrastructural investigations. Invest. Ophthalmol. Vis. Sci. 20 (4), 537–547.
Jester, J.V., Potma, E., Brown, D.J., 2016. PPARγ regulates mouse Meibocyte differentiation and lipid synthesis. Ocul. Surf. 14 (4), 484–494. https://doi.org/10.1016/j.jtos.2016.08.001.
Kostara, C.E., Tsiafoulis, C.G., Bairaktari, E.T., Tsimihodimos, V., 2021. Altered RBC membrane lipidome: a possible etiopathogenic link for the microvascular impairment in Type 2 diabetes. J. Diabet. Complicat. 35 (10), 107998 https://doi.org/10.1016/j.jdiacomp.2021.107998.
Li, L., Gan, H., Jin, H., Fang, Y., Yang, Y., Zhang, J., Hu, X., Chu, L., 2021. Astragaloside IV promotes microglia/macrophages M2 polarization and enhances neurogenesis and angiogenesis through PPARγ pathway after cerebral ischemia/reperfusion injury in rats. Int. Immunopharm. 92, 107335 https://doi.org/10.1016/j.intimp.2020.107335.
Li, P., Shi, L., Shen, H., Sun, X., Gao, W., 2023. Mechanism of EDXKD in relieving ocular surface inflammation of type 2 diabetes related dry eyes in rats based on TH17/IL-17A signaling pathway. Inform. Tradit. Chinese Med. 40 (5), 1–11+31. https://doi.org/10.19656/j.cnki.1002-2406.20230501.
Li, W., Deng, M., Gong, J., Hou, Y., Zhao, L., 2023. Bidirectional regulation of sodium acetate on Macrophage activity and its role in lipid metabolism of hepatocytes. Int. J. Mol. Sci. 24 (6) https://doi.org/10.3390/ijms24065536.
Mastrofrancesco, A., Ottaviani, M., Cardinali, G., Flori, E., Briganti, S., Ludovici, M., Zouboulis, C.C., Lora, V., Camera, E., Picardo, M., 2017. Pharmacological PPARγ modulation regulates sebogenesis and inflammation in SZ95 human sebocytes. Biochem. Pharmacol. 138, 96–106. https://doi.org/10.1016/j.bcp.2017.04.030.
Nelson, J.D., Shimazaki, J., Benitez-del-Castillo, J.M., Craig, J.P., McCulley, J.P., Den, S., Foulks, G.N., 2011. The international workshop on meibomian gland dysfunction: report of the definition and classification subcommittee. Invest. Ophthalmol. Vis. Sci. 52 (4), 1930–1937. https://doi.org/10.1167/iovs.10-6997b.
Ning, N., He, K., Wang, Y., Zou, Z., Wu, H., Li, X., Ye, X., 2015. Hypolipidemic effect and mechanism of palmatine from Coptis chinensis in hamsters fed high-fat diet. Phytother Res. 29 (5), 668–673. https://doi.org/10.1002/ptr.5295.
Nwabueze, O.P., Sharma, M., Balachandran, A., Gaurav, A., Abdul Rani, A.N., Małgorzata, J., Beata, M.M., Lavilla Jr., C.A., Billacura, M.P., 2022. Comparative studies of palmatine with Metformin and Glimepiride on the modulation of insulin dependent signaling pathway in vitro. In Vivo & Ex Vivo. Pharm. (Basel) 15 (11). https://doi.org/10.3390/ph15111317.
Okon, E., Kukula-Koch, W., Jarzab, A., Halasa, M., Stepulak, A., Wawruszak, A., 2020. Advances in Chemistry and Bioactivity of magnoflorine and magnoflorine-containing Extracts. Int. J. Mol. Sci. 21 (4) https://doi.org/10.3390/ijms21041330.
Pan, Z., Chen, X., Wu, D., Li, X., Gao, W., Li, G., Du, G., Zhang, C., Jin, S., Geng, Z., 2023. A Novel in Duck Myoblasts: the transcription factor Retinoid X receptor Alpha (RXRA) inhibits lipid accumulation by promoting CD36 expression. Int. J. Mol. Sci. 24 (2) https://doi.org/10.3390/ijms24021180.
Park, S., Sadanala, K.C., Kim, E.-K., 2015. A Metabolomic Approach to understanding the metabolic link between obesity and diabetes. Mol. Cell. 38 (7), 587–596. https://doi.org/10.14348/molcells.2015.0126.
Phan, M.A.T., Madigan, M.C., Stapleton, F., Willcox, M., Golebiowski, B., 2022. Human meibomian gland epithelial cell culture models: current progress, challenges, and future directions. Ocul. Surf. 23, 96–113. https://doi.org/10.1016/j.jtos.2021.11.012.
Sabeti, S., Kheirkhah, A., Yin, J., Dana, R., 2020. Management of meibomian gland dysfunction: a review. Surv. Ophthalmol. 65 (2), 205–217. https://doi.org/10.1016/j.survophthal.2019.08.007.
Sun, X., Ji, H., Shi, L., Shen, H., Yu, J., Dong, Y., 2024. Clinical efficacy of Erdong Xiaoke decoction in treating type 2 diabetes dry eyes with yin deficiency and heat excess syndrome and its influence on Serum IL-17 and IL-1β. J. Nanjing Univer. Tradit. Chinese Med. (3), 302–308. https://doi.org/10.14148/j.issn.1672-0482.2024.0302.
Tian, Y., Liu, Y., Xue, C., Wang, J., Wang, Y., Xu, J., Li, Z., 2020. Exogenous natural EPA-enriched phosphatidylcholine and phosphatidylethanolamine ameliorate lipid accumulation and insulin resistance via activation of PPARα/γ in mice. Food Funct. 11 (9), 8248–8258. https://doi.org/10.1039/d0fo01219j.
Vernhardsdottir, R.R., Magno, M.S., Hynnekleiv, L., Lagali, N., Dartt, D.A., Vehof, J., Jackson, C.J., Utheim, T.P., 2022. Antibiotic treatment for dry eye disease related to meibomian gland dysfunction and blepharitis - a review. Ocul. Surf. 26, 211–221. https://doi.org/10.1016/j.jtos.2022.08.010.
Villarroel-Vicente, C., Gutiérrez-Palomo, S., Ferri, J., Cortes, D., Cabedo, N., 2021. Natural products and analogs as preventive agents for metabolic syndrome via peroxisome proliferator-activated receptors: an overview. Eur. J. Med. Chem. 221, 113535 https://doi.org/10.1016/j.ejmech.2021.113535.
Wang, H., Zhou, Q., Wan, L., Guo, M., Chen, C., Xue, J., Yang, L., Xie, L., 2021. Lipidomic analysis of meibomian glands from type-1 diabetes mouse model and preliminary studies of potential mechanism. Exp. Eye Res. 210, 108710 https://doi.org/10.1016/j.exer.2021.108710.
Wang, L., Yan, N., Zhang, M., Pan, R., Dang, Y., Niu, Y., 2022. The association between blood glucose levels and lipids or lipid ratios in type 2 diabetes patients: a cross-sectional study. Front. Endocrinol. 13, 969080 https://doi.org/10.3389/fendo.2022.969080.
Wu, H., Lin, L., Du, X., Zhang, L., Yin, X., Dong, X., Hao, X., Xie, L., Qu, C., Ni, J., 2020. Study on the potential effective ingredients of Xiaosheng prescription for dry eye disease. Biomed. Pharmacother. 127, 110051 https://doi.org/10.1016/j.biopha.2020.110051.
Yang, Q., Li, B., Sheng, M., 2021. Meibum lipid composition in type 2 diabetics with dry eye. Exp. Eye Res. 206, 108522 https://doi.org/10.1016/j.exer.2021.108522.
Yu, J., Shi, L., Shen, X., Zhao, Y., 2019. UCP2 regulates cholangiocarcinoma cell plasticity via mitochondria-to-AMPK signals. Biochem. Pharmacol. 166, 174–184. https://doi.org/10.1016/j.bcp.2019.05.017.
Yu, T., Han, X.G., Gao, Y., Song, A.P., Dang, G.F., 2019. Morphological and cytological changes of meibomian glands in patients with type 2 diabetes mellitus. Int. J. Ophthalmol. 12 (9), 1415–1419. https://doi.org/10.18240/ijo.2019.09.07.
Zhang, C., Yu, H., Ye, J., Tong, H., Wang, M., Sun, G., 2023. Ginsenoside Rg3 protects against diabetic cardiomyopathy and promotes adiponectin signaling via activation of PPAR-γ. Int. J. Mol. Sci. 24 (23) https://doi.org/10.3390/ijms242316736.
Zhao, Z., Ukidve, A., Kim, J., Mitragotri, S., 2020. Targeting strategies for tissue-specific drug delivery. Cell 181 (1), 151–167. https://doi.org/10.1016/j.cell.2020.02.001.
Zheng, M., Lee, S., Tsuzuki, S., Inoue, K., Masuda, D., Yamashita, S., Iwanaga, T., 2016. Immunohistochemical localization of fatty acid transporters and MCT1 in the sebaceous glands of mouse skin. Biomed. Res. 37 (4), 265–270. https://doi.org/10.2220/biomedres.37.265.
Zhou, Y., Wang, Y., Vong, C.T., Zhu, Y., Xu, B., Ruan, C.C., Wang, Y., Cheang, W.S., 2022. Jatrorrhizine improves endothelial function in diabetes and obesity through suppression of endoplasmic reticulum stress. Int. J. Mol. Sci. 23 (20) https://doi.org/10.3390/ijms232012064.
Zhu, W., 2020. Clinical Study on the Treatment of Type 2 Diabetic Dry Eyes with Yin Deficiency and Heat Exuberance Type by Er-Dong-Xiao-Ke Decoction and its Effect on MMP-9. Nanjing University of Chinese Medicine. https://doi.org/10.27253/d.cnki.gnjzu.2020.000347.
Ziemke, F., Mantzoros, C.S., 2010. Adiponectin in insulin resistance: lessons from translational research. Am. J. Clin. Nutr. 91 (1), 258s–261s. https://doi.org/10.3945/ajcn.2009.28449C.
Zou, Z., Wang, H., Zhang, B., Zhang, Z., Chen, R., Yang, L., 2022. Inhibition of Gli1 suppressed hyperglycemia-induced meibomian gland dysfunction by promoting pparγ expression. Biomed. Pharmacother. 151, 113109 https://doi.org/10.1016/j.biopha.2022.113109.